Applied Geochemistry 189 (2025) 106432

Contents lists available at ScienceDirect

Applied Geochemistry

journal homepage: www.elsevier.com/locate/apgeochem

Regional geochemical survey of Canadian Arctic sediments: insights into provenance, sediment dynamics and trace metal enrichment

Camille Brice [a,*], Jean-Carlos Montero-Serrano [a], Richard Saint-Louis [b]

[a] Institut des Sciences de la mer (ISMER), Université du Québec à Rimouski (UQAR), Geotop & Québec-Océan, 310 Allée des Ursulines, Rimouski, QC, G5L 3A1, Canada
[b] Université du Québec à Rimouski (UQAR), Département de biologie, chimie et géographie, EcotoQ & Québec-Océan, 300 Allée des Ursulines, Rimouski, QC, G5L 3A1, Canada

ARTICLE INFO

Editorial Handling by: Dr. Zimeng Wang

Keywords:
Marine surface sediment
Major and trace elements
Energy dispersive X-ray fluorescence
Sediment dynamics
Pollution indices
Canadian Arctic

ABSTRACT

Major and trace element contents, grain size distribution and total organic carbon contents were measured in 141 marine surface and terrestrial sediment samples to study modern sediment dynamics in the Canadian Arctic (CA) and to provide an assessment of metal enrichment for V, Zn, Mn and Fe. Samples were collected from different areas between Baffin Bay and the Beaufort Sea during the ArcticNet 2016–2022 expeditions onboard the Canadian Coast Guard icebreaker Amundsen. Geochemical data combined with multivariate statistical analyses allowed the division of the CA into three chemical clusters (CC) and four regional provinces. Central CA (CC#1) and southeastern CA (CC#2) are mainly composed of relatively coarse sediments rich in detrital carbonates (Ca, Mg) and siliciclastic elements (Si, K, Zr), respectively, reflecting coastal erosion of surrounding land (e.g., Victoria Island, Baffin Island) and transport of sediment-laden sea ice. The sediments of CC#3, comprising western and eastern CA, are characterized by organic carbon and Fe–Mn oxyhydroxides. Western CA, which is also characterized by fine-grained aluminosilicates, is influenced by the Mackenzie River discharge, while eastern CA is shaped by polynyas and glacial erosion. The highest concentrations of V and Zn are recorded in the western CA. Over the whole region, significant positive correlations of Al with Zn, V and Fe suggest that lithogenic-derived inputs influence the distribution of these metals in sediments from the CA and that Fe oxides represent the main carrier phase. In western CA, Mn displays positive but weaker relationships with Al and Fe, suggesting a mixed source of Mn oxyhydroxides linked to both detrital fractions and authigenic processes near the sediment-water interface. High terrestrial Mn oxyhydroxide inputs from the Mackenzie River are remobilized and transported to areas with lower oxygen consumption in sediment, i.e., the Amundsen Gulf and Banks Island coasts, which leads to surface sediment enrichment in Mn. The enrichment factor and the geo-accumulation index, two pollution indices commonly used for identifying anthropogenic metal inputs, were also studied to evaluate their suitability in the context of this study. Discrepancies from the normalization of metals with a geochemical background and a normalizing element revealed that pollution indices should be used with caution. Overall, according to the pollution indices and the regional survey, the surface sediments of the CA show minor enrichment in trace metals and thus present natural concentrations relative to regional background values.

1. Introduction

Trace metals naturally occur in the environment, and some are essential elements for biological systems. However, some of them, also known as heavy metals, have become contaminants of concern affecting all systems (AMAP, 1998, 2005), including aquatic environments, because human activities disrupt their natural cycles (Macdonald and Bewers, 1996). Arctic coastal environments and shelves are particularly important areas for biogeochemical cycles and are recognized as regions that are naturally rich in trace elements (Stein and Macdonald, 2004). High inputs of land-derived dissolved and particulate trace elements make these areas sensitive to metal enrichment (Brown et al., 2020; Colombo et al., 2019; Jensen and Colombo, 2024). Indeed, scavenging of dissolved trace metals from the water column to sediments by adsorption, precipitation or complexation with mineral phases (such as clays), Fe-organic colloids, particulate organic carbon and Fe–Mn oxyhydroxide coatings can be very high in the Arctic Ocean (Jensen and Colombo, 2024), making sediments a major sink for those metals.

* Corresponding author.
E-mail address: camille.brice@hotmail.com (C. Brice).

https://doi.org/10.1016/j.apgeochem.2025.106432
Received 23 October 2024; Received in revised form 15 May 2025; Accepted 17 May 2025
Available online 19 May 2025

Despite limited human settlements in the Arctic, and thus limited localized direct anthropogenic trace metal emissions, Arctic environments are nonetheless affected by important inputs of inorganic (e.g., Hg, Pb, and Cd) and organic (e.g., polycyclic aromatic hydrocarbons and persistent synthetic organic compounds) contaminants via long-range atmospheric transport (AMAP, 2005, 2021a, 2021b), making anthropogenic emissions a substantial source of trace metals in the region.

Properly assessing trace metal contamination in Arctic marine sediments requires a clear understanding of the natural geochemical variability across the region. Therefore, analyses of sediment provenance, transport pathways, and depositional conditions are essential, as they establish the geochemical and sedimentological framework needed to distinguish natural background levels from potential anthropogenic inputs (Loring, 1991; Domingo et al., 2023). Studies on the trace metal concentrations and sediment dynamics in Arctic Ocean have been performed in Chukchi and Beaufort seas and Siberian Shelf (e.g., Budko et al., 2022; Crecelius et al., 1991; Kondo et al., 2016; Myers and Darby, 2022; Naidu et al., 2012; Trefry and Neff, 2019; Viscosi-Shirley et al., 2003; Zhang et al., 2021) and in Canadian Arctic rivers (Brown et al., 2020; Colombo et al., 2019; Grenier et al., 2022). However, the vast network of channels, continental shelves, and slopes within the CA remains comparatively understudied (e.g., Deschamps et al., 2018; Gamboa et al., 2017; Kutos et al., 2021; Kuzyk et al., 2017; Letaïef et al., 2021). The spatial distribution of major and trace metals in surface sediments within the CA is influenced by a complex interplay of factors, including the diversity of surrounding geological provinces, the nature of terrigenous source material, the grain size variability, and the presence of geochemical carriers such as metallic oxides and organic matter (Letaïef et al., 2021). These factors, governed by sediment provenance and transport dynamics, ultimately control the natural variability of trace metal concentrations and must be accounted for when evaluating potential contamination (e.g., Domingo et al., 2023).

Chemical pollution indices are a widespread technique for assessing the level and impact of sediment contamination by metals, and discerning the human impacts (e.g., Reimann and de Caritat, 2000). These indices attribute a value that reflects the level of pollution in the sample by normalizing the elements to a natural geochemical background and a conservative element. Even though the pollution indices have been used in multiple environmental studies, the concept of normalization has been questioned because of the natural variability of chemical composition of the natural background and geochemical processes (e.g., redox conditions and bottom scavenging) modify elemental concentrations (Anderson and Kravitz, 2010; Desaules, 2012; Poh and Tahir, 2017; Reimann and de Caritat, 2000, 2005; Tribovillard et al., 2006; Van der Weijden, 2002).

In this context, major and trace elements content, grain size and total organic carbon (TOC) content were measured in this study on marine surface and terrestrial sediment samples from the CA to (1) establish a portrait of the spatial regional variability of the chemical composition of the seafloor, (2) acquire a better understanding of the sediment provenance and the sedimentary and geochemical processes that govern the distributions of major and trace elements, and (3) evaluate the applicability of commonly used pollution indices for assessing trace metal enrichment in surface sediments. Additionally, this study provides a geochemical baseline and contribute to a comprehensive understanding of sediment transport processes that operate across the Canadian Arctic.

2. Study area

The study area comprises the Canadian mainland north of 65°N and the Archipelago, a network of islands, and narrow and shallow channels connecting the Arctic Ocean to the Labrador Sea (Fig. 1). It is entirely covered by a continued permafrost (Heginbottom et al., 1995), which stores large amounts of soil organic carbon, especially in the western part of the CA (Hugelius et al., 2014). Hydrology is restricted and controlled by seasonal freezing and thawing of the permafrost. Located on the western coast of the mainland (Fig. 1), the Mackenzie River is the most important river of the CA. It drains an area of approximately 1.78 $\times$ 10^6 km^2 and has a mean discharge of ~300 km^3/yr (Millot et al., 2003). It is also the largest Arctic river in terms of suspended sediment flux and the second largest in terms of dissolved material to the Arctic Ocean (Millot et al., 2003). Smaller rivers also contribute significantly to

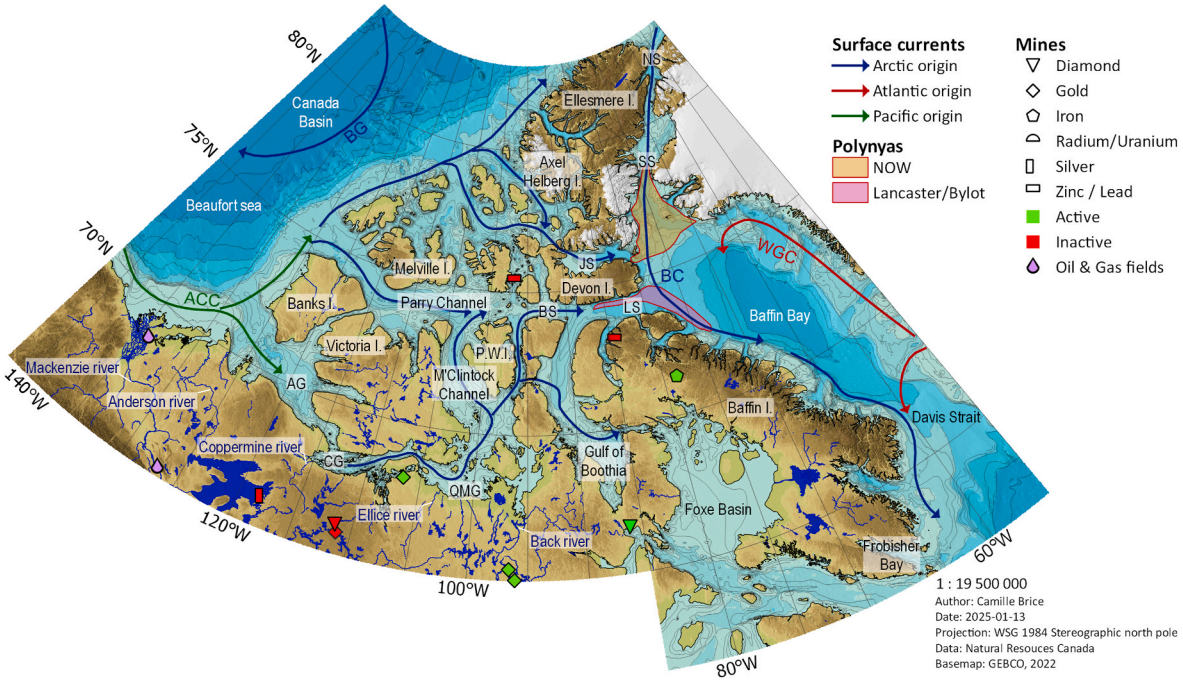

Fig. 1. Map of the Canadian Arctic showing the main geographical setting, i.e., surface currents, polynyas and active and abandoned mines and gas/oil fields. AG: Amundsen Gulf, BS: Barrow Strait, CG: Coronation Gulf, JS: Jones Sound, LS: Lancaster Sound, NS: Nares Strait, QMG: Queen Maud Gulf and SS: Smith Sound. ACC: Alaska Coastal Current, BC: Baffin Current, BG: Beaufort Gyre and WGC: West Greenland Current. P.W.I.: Prince of Wales Island.

the global discharge in central CA (Fig. 1), with an annual discharge estimated to be ~260 km^3/yr (Alkire et al., 2017). This includes the Coppermine River, whose outlet is situated in the community of Kugluktuk (~8.77 km^3/yr), the Ellice River (~2.82 km^3/yr), the Back River (~15.52 km^3/yr) and the Anderson River (~4.72 km^3/yr; Déry et al., 2016).

Within the CA, three water masses are found (McLaughlin et al., 2005; Steele et al., 2004): the Polar Mixed Layer (PML), the Arctic waters of Pacific origin (ApW) and the Atlantic waters (AW). The PML is found in the upper 50–100 m of the water column and consists of summer meltwater and river discharge. The ApW occupy the 100–300 m water depth layer. It is a fresh and nutrient-rich water mass dominating the western CA that flows eastward along the coast via the Alaska Coastal Current (ACC; Fig. 1). The saline and warmer AW are found beneath the ApW in the Canada Basin and in the Baffin Bay. The shallow channels in central CA are composed of only the first two water masses. A prevailing west-east current flows through the islands of the Canadian Arctic, transporting Arctic and Pacific waters eastward toward the Atlantic, propelled by the elevated sea level in the Pacific. Sea ice completely covers the CA waters seasonally, with freeze-up starting in September and break-up starting in June (Canadian Ice Services, 2023). First-year sea ice is predominant in the CA and covers most of the area, except in areas such as the northern Beaufort Sea and channels north of the Parry Channel, where old ice predominates (Canadian Ice Services, 2023). Freshet from the Mackenzie River combined with wind and summer temperatures lead to ice-free waters on the Beaufort Shelf and slope in July/August (O'Brien et al., 2006). Multiple polynyas are present in Canadian Arctic waters, namely the well-known North Water Polynya (NOW; Pikialasorsuaq), and the Lancaster Sound and Bylot Island Polynyas (Fig. 1; Stirling and Cleator, 1981; Hannah et al., 2009). They are maintained by latent heat and ice arches formed in the Nares Strait and Lancaster Sound (Vincent, 2023). These polynyas, especially the Pikialasorsuaq, are highly productive areas (Ribeiro et al., 2021) with high resulting fluxes of organic carbon (Hamel et al., 2002).

Three main regional geological units characterize the CA: the Canadian Shield, the Interior Plains and the Innuitian Orogen (Fig. 2; Brown, 1972; Harrison et al., 2011). The Canadian Shield, which occupies the eastern part of the study area, is divided into the provinces of Churchill, Bear and Slave, and is mainly composed of Archean and Proterozoic gneiss, granites and gabbros (Harrison et al., 2011). Younger interior and Arctic platforms form the Interior Plains, which are made up of carbonate rocks, mostly dolostones, in central CA and sedimentary rocks, such as siltstone and sandstone, in western CA. The Silurian-Devonian Innuitian Orogen consists of mildly to strongly folded and deformed sedimentary units (Harrison et al., 2011; Trettin et al., 1989). It occupies the islands of northern CA, i.e., the Queen Elizabeth Islands.

Modern sedimentary processes across the CA are dominated by river discharge, entrainment by sea ice, and coastal and glacial erosion (Letaïef et al., 2021). The Mackenzie River, along with the small rivers of the CA, are exporting significant amounts of land-derived inorganic and organic material to the ocean originating from the surrounding geology, i.e., Precambrian igneous and metamorphic rocks to central and eastern CA and younger sedimentary rock to western CA (Millot et al., 2003). The erosion of Arctic coasts and the resulting sediment inputs are substantial, mainly because of permafrost thaw. On average, Arctic coastal erosion rate is 0.5 m.yr^{-1}, though rates can exceed 3 m.yr^{-1} along the Beaufort Sea coast. This process contributes to significant fluxes of material, including contaminants, to the marine environment (Lantuit et al., 2012). Although data on coastal erosion within the Canadian Arctic Archipelago remain limited, the existing studies suggest that most coastlines are relatively stable (Lantuit et al., 2012; St-Hilaire-Gravel et al., 2012). Letaïef et al. (2021) however identified coastal erosion as a key driver for sediments transport for the Banks Island area, the M'Clure Strait and the Barrow Strait/Lancaster Sound. Suspended fine-grained sediments coming from rivers and coastal erosion can also be entrained by frazil and anchor ice (Darby et al., 2011; Reimnitz et al., 1993). The incorporation of sediments into sea ice during its formation is an important sedimentary transport process, mainly in the Beaufort Sea. As sea ice is transported by surface currents and subsequently melts, the entrained particles are redistributed, with their presence observed further east, as interpreted by Letaïef et al. (2021). Finally, several glaciers are present along the eastern coasts of Ellesmere, Devon and Baffin Islands, which highly contribute to the sediment supply, mainly in fjords (Normandeau et al., 2019; Syvitski and Normandeau, 2023).

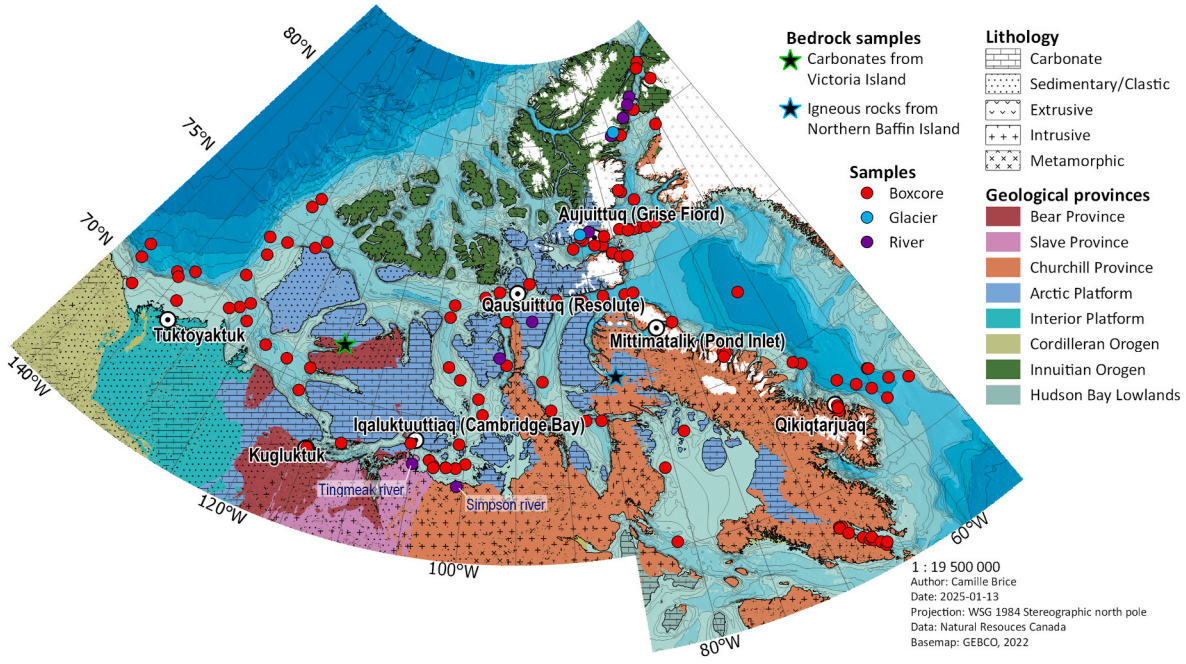

Fig. 2. Geological map of the Canadian Arctic (data from Harrison et al., 2011) with the location of the samples. Comparative bedrock samples include carbonates from Victoria Island (Bédard et al., 2016) and igneous rocks from the Jungersen River in the Churchill Province (Lebeau, 2022).

3. Methodology

3.1. Sampling

A total of 128 surface sediment samples and 13 terrestrial samples (including glacial till and sediments from riverbanks) were collected from different areas between Baffin Bay and the Beaufort Sea as well as in the Nares Strait during the ArcticNet summer expeditions (2016–2019 and 2022) onboard the Canadian Coast Guard Ship (CCGS) icebreaker Amundsen (Fig. 2; Table S1). The terrestrial sampling sites were accessed with the ship helicopter as the CCGS Amundsen traveled through the CA. The marine sediments were sampled with a box corer (50 cm × 50 cm x 60 cm) and the surface uppermost 1 cm of each box core was sampled onboard using a plastic spatula and stored in plastic bags at 4 °C. Push cores (10 cm diameter) were taken from each box core collected during the expeditions; they were subsequently subsampled in the laboratory. The bases (lowermost 1–1.5 cm) of 37 of these push cores were used in this study to establish a regional geochemical background (Table S2). Based on a compilation of sedimentation rates from various studies within the CA (modified from Letaïef et al., 2021), we estimate that the basal sediments of the push cores correspond to pre-industrial times (pre-1900 Common Era or CE; Table S2), and therefore to natural values.

3.2. Laboratory analyses

All samples were analyzed for major and trace element contents and grain size. While most of the TOC data used in this study are from Corminboeuf et al. (2021), additional TOC analyses were performed on new sediment samples to enhance regional coverage, following the same methodology and using the same instrument. For TOC analysis and elemental geochemistry, all samples were first wet-sieved through a 150-μm Nitex® mesh using distilled water and then oven-dried (<60 °C) for 12 h, crushed and homogenized with an agate mortar. The <150 μm fraction includes fine-grained sediments, such as clay, silt and fine sand, which allow not only to avoid spatial biases in elemental concentrations linked to coarse-grained size variations, but also to capture the regional geochemical signature of the environment and the different sediment transport processes operating across the CA.

The total carbon (TC) and TOC contents in the <150 μm sediment fraction were measured at the Geotop Light Stable Isotope Geochemistry Laboratory (Montreal, Quebec) with a Carlo-Erba NC 2500 elemental analyzer following the acidification in solution method described in Hélie (2009). Briefly, each sample was divided into two aliquots. The first one (bulk sediment) was used to determine the TC content. The second aliquot was acidified with 1 M HCl to remove carbonates, dried and milled. This carbonate-free aliquot was used to determine the TOC content. To account for inorganic carbon mass loss, a correction was applied to the results (Hélie, 2009). Analytical precision and accuracy were determined by duplicate analyses of samples and replicate analyses of in-house and international standards (low organic content soil, cyclohexanone-2,4-dinitrophenylhydrazone, atropine and acetanilide) and were better than ±0.02 % (1σ).

Grain size analysis was performed with a Malvern PANalytical Mastersizer 3000 laser diffraction grain size analyzer equipped with a Hydro LV module following the instrumental conditions outlined in Belzile and Montero-Serrano (2022). Before measurement, an aliquot of the bulk fraction of each sediment sample was treated with 5–10 mL 30 % H_2O_2 to remove organic matter. The dry residues were then diluted with ~30 mL of sodium hexametaphosphate (20 % v/v), sieved at <2 mm, and disaggregated using an in-house rotator for 12 h prior to particle size measurements. The grain size data obtained was processed using the GRADISTAT software version 9.1 (Blott and Pye, 2001).

A total of eight major elements (Mg, Al, Si, K, Ca, Ti, Mn, and Fe) and five trace elements (V, Cr, Zn, Sr, and Zr) were measured in the <150 μm sediment fraction using a Malvern PANalytical Epsilon 3-XL energy dispersive X-ray fluorescence spectrometer (ED-XRF). Prior to ED-XRF measurements, the loss on ignition (LOI) was determined gravimetrically by weighing an aliquot of 2 g before and after heating it for 4 h at 950 °C. Following the LOI, ~1.1 g of the ignited samples were mixed with 5.5 g of lithium tetraborate (CLAISSE, pure, 99,00 % $Li_2B_4O_7$, and 1,00 % LiBr) and fused with a CLAISSE M4 Fluxer automated fusion furnace to form glass disks. The glass disks were analyzed for elemental geochemistry with the ED-XRF. The acquired ED-XRF spectra were treated with the Malvern PANalytical Omnian standardless software package calibration, and the acquired data are expressed as percent mass (wt.%) for major elements and micrograms per gram (μg/g) for trace elements. Procedural blanks were prepared with synthesized silicon oxide powder (99.999 % SiO_2; American Elements; SI-OX-05M-P.325 M). The SiO_2 blank concentrations are less than the detection limit (DL; Fig. S1; Table S3) for most major and trace elements, except for Al_2O_3 (~0.83 %; Table S4). This Al contamination is probably derived from the ceramic crucibles used for LOI determination. Thus, the Al concentrations in the sediment samples are corrected by subtracting the mean Al values of the procedural blanks. The accuracy of the overall method, including the digestion and glass disks preparation, was assessed by analyzing the USGS certified material SDC-1 and BCR-2. The results obtained for these reference materials are in good agreement with reference values from the GeoREM database (http://georem.mpch-mainz.gwdg.de/; Fig. S1). Except for MgO in the analysis of SDC-1, the recovery values (accuracy) for all the measured elements were between 91 and 118 % (Table S5), which corresponds to the usual acceptable deviation limits (Thompson et al., 2002). The reproducibility of ED-XRF analysis, based on replicate analysis of USGS standards SDC-1 and BCR-2 every 9 samples, was <8 % relative standard deviation (RSD, 1σ) for major elements, <11 % for V and <5 % for the other elements (Table S5). Cr was excluded from the statistical analysis because the majority of the results were below the DL, and the accuracy with certified material was not acceptable; however, few results were kept as qualitative values in the interpretation.

3.3. Pollution indices

Two pollution indices were used to determine metal pollution/enrichment in the sediment and to assess anthropogenic influence. Different geochemical backgrounds were employed for the calculation of the indices to consider the warnings mentioned by several studies (Reimann and de Caritat, 2000, 2005; Van der Weijden, 2002; Anderson and Kravitz, 2010; Tribovillard et al., 2006; Desaules, 2012; Poh and Tahir, 2017). Three geochemical backgrounds were used in the calculations of the pollution indices for comparison: 1) Average Shale (AS; Turekian and Wedepohl, 1961), 2) Upper Continental Crust (UCC; Taylor and McLennan, 1985), and 3) a regional geochemical background obtained from basal sediment samples from 37 push cores collected in the CA representing pre-industrial times. This pre-industrial background was subdivided into local backgrounds according to the clusters determined with the surface samples. The pollution indices used in the study are as follows, and the pollution classification levels are shown in Table 1:

Enrichment factor - The enrichment factor (EF) is used to determine if there has been an increase in the levels of that element by an anthropogenic contribution using the following equation:

$$EF = \frac{X_{sample}/Y_{sample}}{X_{background}/Y_{background}}$$

where X_{sample} is the concentration of the trace element in the sample and Y_{sample} is the concentration of a normalizing element in the same sample. $X_{background}$ and $Y_{background}$ are the concentrations of the trace element and the normalizing element, respectively, in the geochemical background. Iron and aluminum are both proposed in the literature as normalizing elements (Birch, 2020), but iron is involved in diagenetic

Table 1
Classes of pollution indices used in this study. EF: enrichment factor, Igeo: Geo-accumulation index.

Indice	Classes	Values	Sediment quality	References
EF		EF < 1	No enrichment	Hakanson (1980)
		EF = 1–3	Minor enrichment	
		EF = 3–5	Moderate enrichment	
		EF = 5–25	Moderately severe enrichment	
		EF = 25–50	Very severe enrichment	
		EF > 50	Extremely severe enrichment	
Igeo	0	Igeo <0	Uncontaminated	Müller (1969)
	1	0 < Igeo <1	Uncontaminated to moderately contaminated	
	2	1 < Igeo <2	Moderately contaminated	
	3	2 < Igeo <3	Moderately to heavily contaminated	
	4	3 < Igeo <4	Heavily contaminated	
	5	4 < Igeo <5	Heavily to extremely contaminated	
	6	5 > Igeo	Extremely contaminated	

processes that can lead to its enrichment in the first layers of marine sediment. Also, large land-ocean interactions are rapidly evolving in the Arctic, which impact the iron inputs to coastal marine sediments (Colombo et al., 2021; Jensen and Colombo, 2024; O'Donnell et al., 2024). Thus, to study the biogeochemical processes that influence the metal composition of surface sediment, including iron, another element should be used as the normalizer. Aluminum is the normalizing element used here because it is not affected by direct anthropogenic disturbance and redox conditions, it is a major component of detrital sediments and Al has been used as a normalizing element in previous geochemical studies on the Canadian Arctic Archipelago (Trefry and Neff, 2019). Ti, a frequently used and reliable normalizing element (Boës et al., 2011), was also tested to assess discrepancies with Al (Fig. S4).

Geo-accumulation index - The geo-accumulation index (Igeo) classifies the pollution level of a trace element into seven classes (Müller, 1969), as reported in Table 1. The index is calculated with the following equation:

$$\text{Igeo} = \log_2(\text{Cn}/1.5\text{Bn})$$

where Cn is the concentration in μg/g of the trace element in the sample and Bn is the concentration (μg/g) of that element in the geochemical background. The constant 1.5 is a factor that considers the possible variations in the geochemical background values generated by lithological changes.

3.4. Statistical and spatial approach

Statistical analyses were performed on the ED-XRF data using R software (R Core Team, 2024). A multiplicative lognormal imputation (Palarea-Albaladejo and Martín-Fernández, 2013, 2015) was implemented to impute values below the DL of the data. Prior to multivariate analysis, a centered-log ratio (clr) transformation was applied to remove the statistical constraints on the compositional data (Aitchison, 1982) using the R package "compositions" (van den Boogaart and Tolosana-Delgado, 2008). A K-means clustering analysis was performed with ED-XRF, LOI and TOC data to group samples with similar chemical compositions within the CA. The cluster analysis was conducted with the R package "stats" (R Core Team, 2024). The quality of the analysis was evaluate using a silhouette plot ("factoextra" R package; Kassambara and Mundt, 2020), where negative values indicate an incorrect and/or questionable assignment (Borcard et al., 2011). Principal component analysis (PCA) was performed with the package "FactoMineR" (Lê et al., 2008) to identify elemental associations with similar relative variation patterns and to extract common trends between all variables and clusters. A Spearman correlation matrix was also applied to data, using the package 'corrplot' (Wei et al., 2017) to compare major and trace elements with D_{90} particle size, LOI and TOC data. Nonsignificant correlation coefficients (p-value >0.05) are not shown in the matrix. Geochemical distribution maps were generated using QGIS version 3.22.10.

4. Results and interpretations

The elemental concentration revealed significant spatial variation within the CA. Values for major elements ranged from 0.2 to 11 wt % for Mg, 0.6 to 9 wt % for Al, 3 to 38 wt % for Si, 0.1 to 21 wt % for Ca, 0.3 to 6 wt % for Fe, and 0.01 to 2 wt % for Mn (Fig. 3). The LOI also presents important variability, with values ranging from 2 to 43 %. Central CA and Foxe Basin are marked by the highest values for Mg and Ca and the lowest values for Fe, Al and Si, while the Beaufort Sea and Baffin Bay areas roughly show opposite results. High Mn contents in sediment are observed in Amundsen Gulf and in northern Davis Strait. For trace elements, V shows high variability, with concentrations ranging from <50 (DL) to 306 μg/g, with the highest concentrations found in samples located from the Beaufort Sea and the Amundsen Gulf. Most samples had Cr concentrations < 100 μg/g (DL), but some samples from the Beaufort Sea, Amundsen Gulf and Baffin Bay recorded concentrations between 100 and 135 μg/g.

The texture of the sediments (<150 μm fraction) found in the CA range from silt, sandy silt and silty sand (Fig. S2), which is consistent with previous regional studies performed from the Beaufort Shelf to Baffin Bay (e.g., Crecelius et al., 1991; Gamboa et al., 2017; Loring, 1984; Letaïef et al., 2021; Corminboeuf et al., 2021). The D_{90} for the <150 μm fraction ranges from 12 to 212 μm, with a west-east increasing trend (Fig. 4a). The Beaufort Sea, and the Amundsen and Coronation Gulfs are mostly composed of fine silt. A mix of fine to coarse silt characterizes the Queen Maud Gulf and central channels. The grain size in Baffin Bay and Nares Strait varies from fine silt to fine sand, depending on the proximity to the coast and water depth. The coarsest material, i.e., very coarse silt to fine sand, is found in Frobisher Bay and Baffin Island fjords.

The TOC content ranges from 0.1 to 2 % throughout the CA, with higher concentrations observed in the fine-grained sediment samples (silt; Fig. 4b & S2). The highest TOC content is found in Jones Sound, Lancaster Sound and Smith Sound, with concentrations around 1–2 %. A gradient is observed in the TOC content in Western CA, with values reaching 2 % close to the Mackenzie River mouth and decreasing when moving away from it, i.e., to 0.4 % north of Banks Island and 0.7 % in Amundsen Gulf. Frobisher Bay samples have values varying from 0.2 to 2 % and show an unclear decreasing trend from the inner to the outer bay. The TOC content in Baffin Bay is within the same values range. The samples from Baffin Bay fjords have low values and those from Davis Strait have values around 0.7–1 %. The lowest concentrations are measured in the Foxe Basin and northern Nares Strait. In terrestrial samples, the TOC content varies between 0.1 and 9 %, with the highest content found in proglacial rivers and glaciers of southern Ellesmere Island.

K-means cluster analysis revealed that the marine surface sediment samples in the CA can be divided into three chemical clusters (CC). A geographical component is clearly observable in the distribution of the

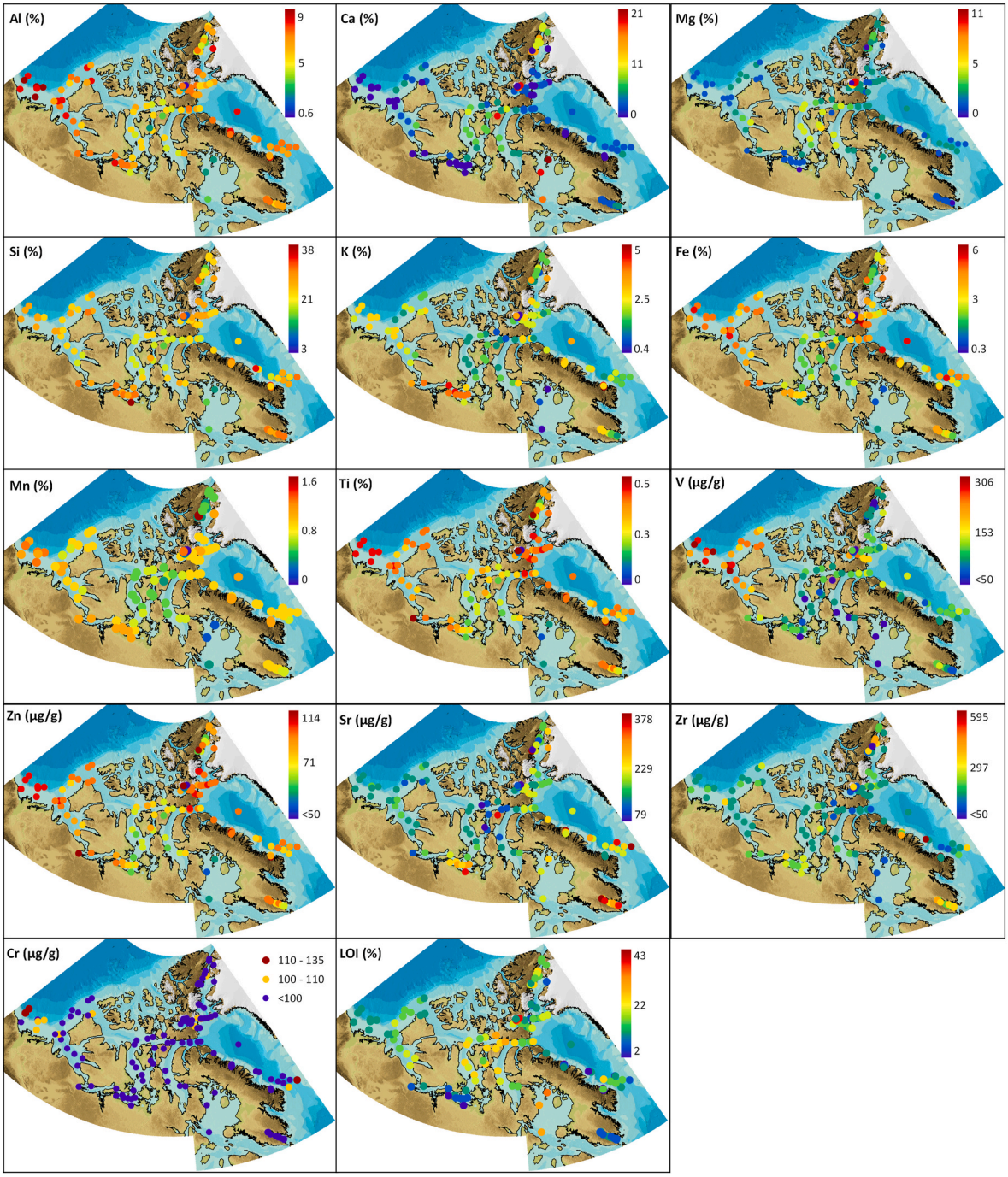

Fig. 3. Distribution map of major elements (in wt.%) and trace elements (in µg/g) in surface marine and terrestrial sediments of the CA. Fig. 1 presents the geographical information.

clusters within the CA (Fig. 5a). Except for two samples, the clustering analysis correctly classified all the samples according to the silhouette plot (Fig. 5b). The first CC regrouped samples in central CA, i.e., Barrow Strait, M'Clintock Channel, Gulf of Boothia, Foxe Basin, and northern Nares Strait. CC #2 consists of samples located in eastern Baffin Island fjords and Frobisher Bay, and Coronation and Queen Maud Gulfs. The third and largest CC can be subdivided into two parts: western and eastern CA. Western CA is represented by samples originating from the Beaufort Sea, western Banks Island Coast and Amundsen Gulf, whereas eastern CA is mostly represented by samples located around Lancaster and Jones Sounds, and Baffin Bay (south of Smith Sound and north of the Davis Strait). PCA based on ED-XRF, LOI and TOC data indicates that the first two principal components (PC) explain 79 % of the total variance (Fig. 6a). PC1 scores (52 % of the total variance) are positively associated with Ca–Mg-LOI, whereas PC2 scores (27 % of the total variance) are positively associated with Zr–Sr–Si–K–Al and negatively associated with TOC-V-Fe and Mg-LOI (Fig. 6b). The samples are presented in the biplot as points with size varying according to their grain size, which reveals that PC2 scores are mostly associated with coarse-grained sediments. Mn was not included in the PCA because of its strong influence on elemental geochemical variability. The three clusters determined were clearly distinct in the biplot. Samples in CC#1 are all located on the positive side of PC1 with Ca, the samples in CC#2 are grouped in positive PC2, where coarse-grained sediments are predominant, and the

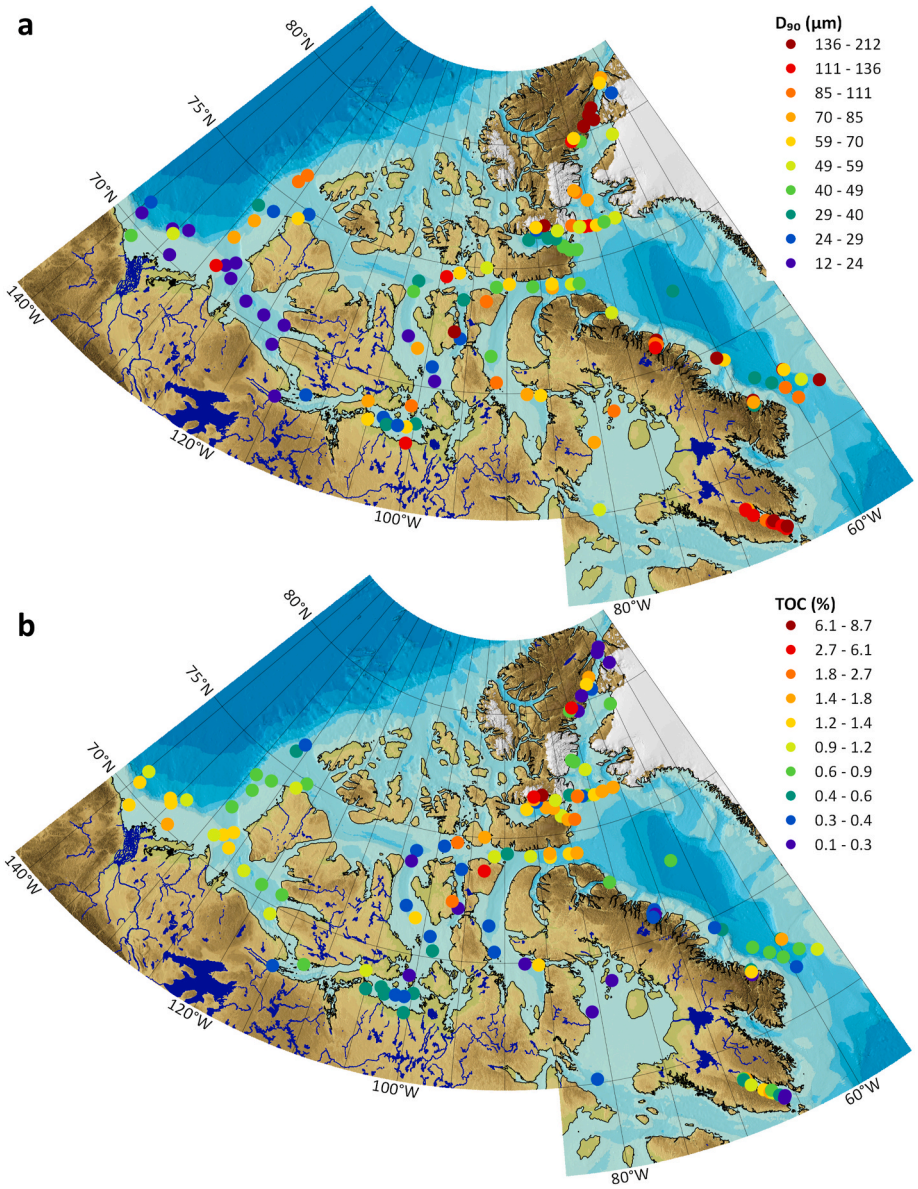

Fig. 4. (a) Distribution map of sediment grain size in µm. (b) Distribution map of the total organic carbon content in %. Fig. 1 presents the geographical information.

samples in CC#3 are roughly situated in the negative PC1/negative PC2 quadrant.

For all clusters, the Spearman rank correlation matrix (Fig. 7a) shows a negative correlation of all elements except Sr, Si and Zr, with D_{90}, suggesting that they are more concentrated in the fine-grained fraction (silt). In contrast, Si and Zr are indicators of coarse-grained sediments (sandy silt and silty sand; Rothwell and Croudace, 2015). Al and Ti are closely correlated with each other (0.71), and with K (0.77 and 0.55), Fe (0.79 and 0.77) and V (0.62 and 0.68), which suggests that lithogenic-derived inputs influence the distribution of these elements (Askari-Dehno et al., 2022; Choudhary et al., 2023; Rothwell and Croudace, 2015). However, the moderate positive correlations of Mn with Al (0.55), Fe (0.55) and the absence of correlation with Ti may indicate that Mn likely derives from both continental and authigenic sources (Macdonald and Gobeil, 2012). As shown in Fig. 7b, the correlation between Mn and Fe can be divided into two main types reflecting the two sources. The light gray circle highlights a linear Fe–Mn relationship, indicating lithogenic provenance, which is observable in all the clusters, except for some CC#3 samples. These samples, mainly from the Amundsen Gulf and Baffin Bay (dark gray circles), exhibit authigenic Mn enrichment. The observed positive correlations of V and Zn with Fe (0.85 and 0.49) and with Al (0.62 and 0.47) suggest that their distributions are partly associated with aluminosilicates but are mainly controlled by adsorption onto Fe oxides (Choudhary et al., 2023). Organic matter accumulation seems also to be an important process influencing V sedimentation, as shown by the positive correlation between V and TOC. Ca, Mg and LOI present good positive correlations, highlighting their association with detrital carbonates.

The Si–Ca–Al ternary plot (Fig. 8) shows that the CC#2 and CC#3 samples consist of detrital material similar to UCC and AS, whereas CC#1 samples plot along a mixing trend between UCC/AS values, Nares Strait sediment composition (Caron et al., 2020) and the carbonate endmember (Bédard et al., 2016). Compared with CC#3, CC#2 is slightly enriched in Si, which is consistent with the composition of the UCC and the igneous rocks from the Jungersen River (Lebeau, 2022), as well as the sediments from Baffin Bay (Loring, 1991). In contrast, CC#3 exhibits a higher Al content than CC#2 and shows a chemical composition similar to suspended sediment samples from the Mackenzie River Basin (Dellinger et al., 2017), Mackenzie Shelf sediments (Gamboa et al., 2017) and AS.

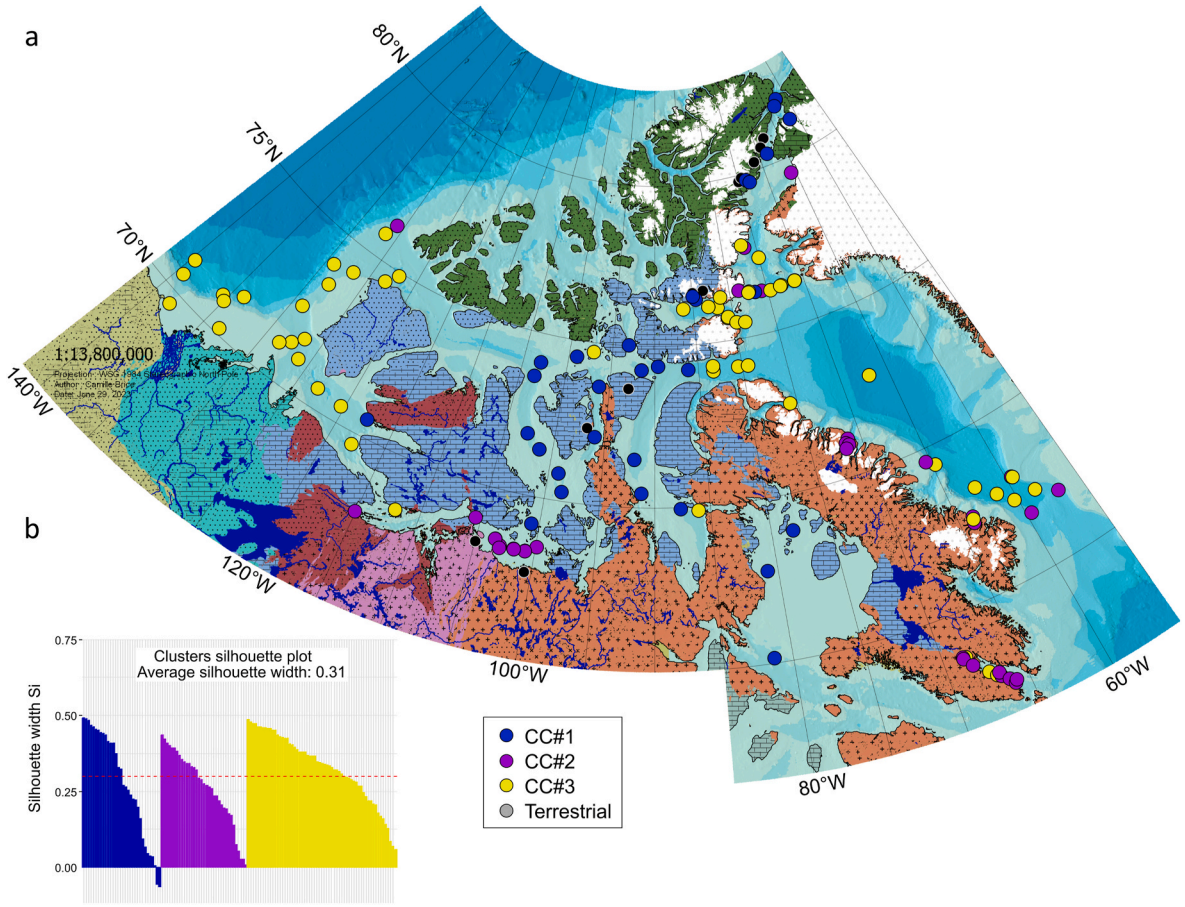

Fig. 5. (a) Map showing the repartition of the three chemical clusters. (b) Silhouette plot resulting from the K-means clustering analysis of the marine surface sediments. Fig. 1 shows the geographical information.

Compared with all three background levels, the EF and Igeo indices indicated that there was no significant enrichment or pollution in Zn or Fe. However, there are some indications of enrichment in V and Mn (Fig. 9). With the UCC values as background, moderately severe enrichment in V is observed in four samples: two river samples from southern Ellesmere Island (EF = 18 and 8; Fig. S4a) and two marine surface samples from the Amundsen Gulf and southern Banks Island (EF = 5.4 and 5.2, respectively). The reason for such high EF results in terrestrial samples is the very low Al content rather than the high V content. All the samples from the Beaufort Sea and Amundsen Gulf, and most of the samples from Jones Sound present moderate enrichment. When the AS values were used as the background, the EF values decreased significantly compared with those of the UCC, with only the river samples showing enrichment in V. The EF values, when the chemical composition of the base of push cores were used as the background, revealed no to minor enrichment of V–Zn–Mn–Fe.

According to the Igeo with UCC as background, sediment samples from the Beaufort Sea and Amundsen Gulf are moderately polluted in V, along with two samples from central Jones Sound. The two river samples from southern Ellesmere Island show unpolluted levels (Fig. S4a). When the AS values were used as the background, Igeo values differ, with values significantly lower (Fig. 9). Without indicating any polluted samples, the Igeo values with the basal samples from the push cores as background are generally higher for Zn and Fe than for the AS and UCC values.

Regardless of the geochemical background used to calculate the EF, dozens of samples present moderate to moderately severe enrichment in Mn throughout the CA, mainly south of the Parry Channel (Fig. 9 and S3). Amundsen Gulf and Davis Strait contain the largest number of moderately severely enriched samples in Mn. Similar results are observed with Igeo, with samples classified as moderately to strongly polluted.

5. Discussion

5.1. Spatial variability and sediment provenance

A large regional variability is observed in the chemical composition of surface sediments across the CA. The three chemical clusters identified four spatial zones in the study area: CC#1 occupying central CA, CC#2 in southeastern CA, and CC#3 subdivided into western CA and eastern CA.

The samples from CC#1 in central CA present sediment rich in calcite and dolomite (Belt et al., 2010; Lakeman et al., 2018; Myers and Darby, 2022). The 32 samples found in this cluster are associated with detrital carbonates derived from the erosion of the dolostone of the Arctic platform and the limestone from the Innuitian Orogen in northern CA. These rocks are predominant in multiples islands in central CA, such as Victoria, Prince of Wales, Devon Islands (Figs. 1 and 2). It is therefore reasonable to conclude that the surrounding geology is the main source for Ca and Mg in the central CA cluster. However, the notable variability observed in grain size and Al–Si content in CC#1 (Figs. 4 and 8) indicates that different transport processes are affecting the distribution of sediment. The sediments with the coarsest grain size combined with the lowest Al content and highest Ca–Mg content are observed in Nares Strait, Gulf of Boothia, Foxe Basin, where coastal erosion of nearby carbonate bedrock predominates. The presence of finer sediments enriched in Al in Lancaster Sound and M'Clintock Channel suggests a

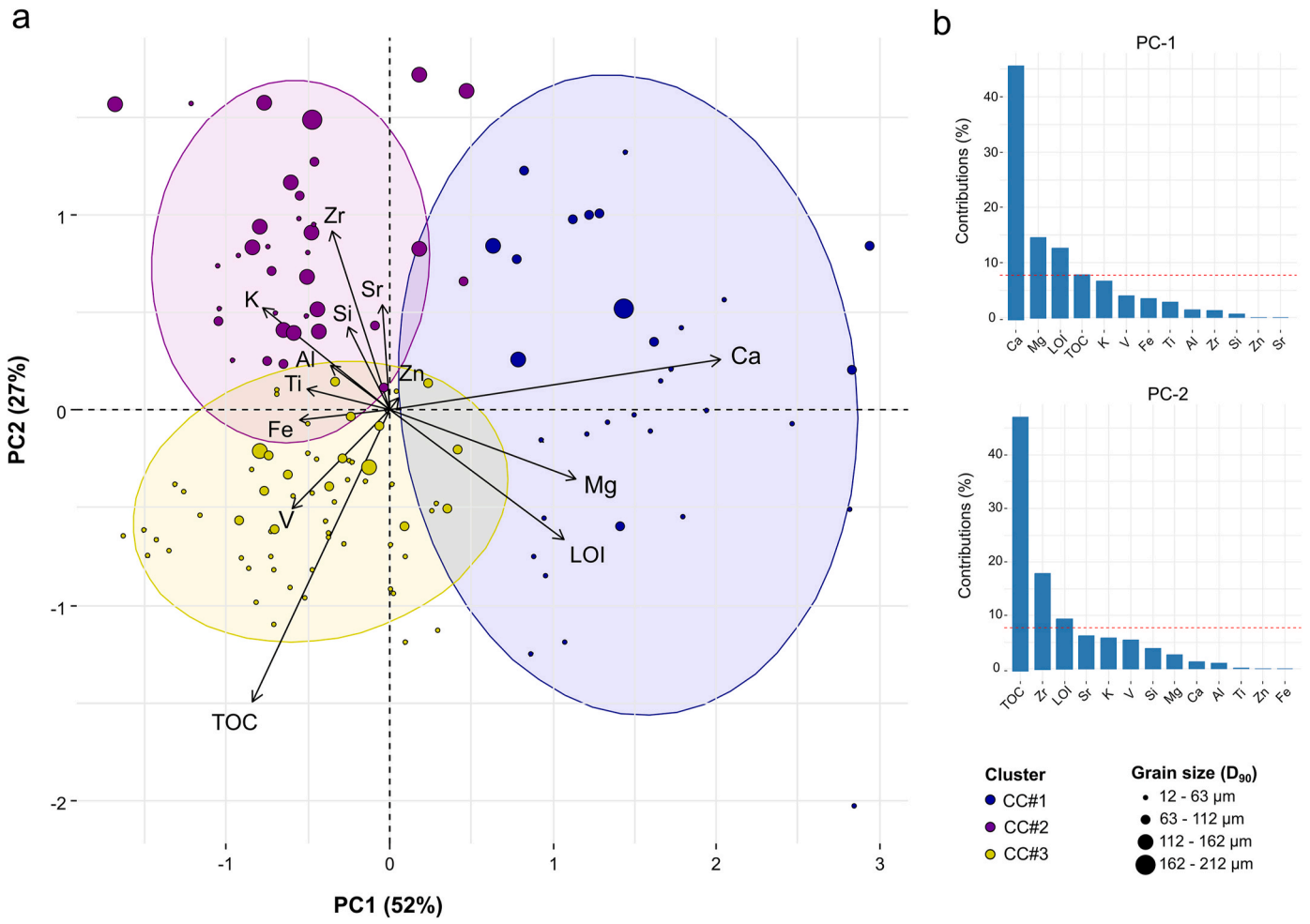

Fig. 6. (a) Biplot of the first and second principal components of the principal component analysis obtained from the ED-XRF, LOI and TOC data. The color of the individuals represents the associated cluster and size of the individuals represents their grain size (D_{90}). Colored ellipses were generated assuming a multivariate t-distribution. (b) Contribution of all variables to the first and second principal components. The red dashed line on the graph above indicates the expected average contribution. (For interpretation of the references to color in this figure legend, the reader is referred to the Web version of this article.)

more distant source. The sediments are slightly better sorted but, though still classified as poorly sorted (Fig. S5), indicating that they are likely transported by surface currents flowing northward from the Amundsen Gulf and eastward through Barrow Strait (Fig. 1), as well as by drifting sea ice. Indeed, sediment-laden sea ice is an important process in the Arctic Ocean that transports fine particles over long distances (Reimnitz et al., 1993), which was also observed by Letaïef et al. (2021) in Lancaster Sound and M'Clure Strait. The negative correlation between Ca–Mg-LOI and Al, along with all the other variables (Fig. 7a), demonstrates that detrital carbonate sediments and aluminosilicates originate from distinct regions. These findings also reveal that these sediments are poor trace metal carriers.

CC#2, in the southeastern CA region, includes Coronation and Queen Maud Gulfs, eastern Baffin Island fjords and Frobisher Bay. This cluster is characterized by elements (Al, Si, K, Sr and Zr; Figs. 6 and 8) that can be associated with K-feldspar, illite, quartz and zircon (Gamboa et al., 2017). Zr contributes greatly to the total variance in this cluster, as shown in the biplot (Fig. 6). This element, which is a ubiquitous mineral in the crust and occurs in zircon grains in igneous and sedimentary rocks, is a coarse grain size indicator (Rothwell and Croudace, 2015). In addition to terrestrial sediments, this cluster is indeed composed of the coarsest sediment of the dataset (sandy silt to silty sand; Fig. S2), with finer sediments found in the Queen Maud Gulf and coarser sediment found in eastern Baffin Island fjords and Frobisher Bay. Proximity of the samples to the coast and to the Canadian Shield rocks explains the composition of this cluster. For example, Queen Maud Gulf sediments are particularly rich in Si (25–30 %, Fig. 8) and K (3.5–4.0 %), which is similar to the Tingmeak and Simpson Rivers (Si: 29 % and K: 3.7 %, and Si: 38 % and K: 2.4 %, respectively), draining granitoid rocks form the Slave and Churchill Provinces (McMartin et al., 2013). Letaïef et al. (2021) reported similar results in Coronation and Queen Maud Gulfs, with dominant content of Si–Al–Zr–Sr–K. As suggested by these authors, the local seafloor of these gulfs is primarily fed by sediments from surrounding rivers (such as Coppermine in Coronation Gulf and Back, Hayes, Perry, Armark, Simpson, Hayes and Ellice rivers in Queen Maud Gulf; Alkire et al., 2017) draining the Canadian Shield and flowing northward to the gulfs, but also by sea ice transport that contributes finer sediments (Belt et al., 2010). The sediments from Baffin Island fjords mostly originated from glacial erosion of Precambrian granites and gneiss from tidewater glaciers. Sandy gravity flows resulting from summer chute failures at the fjord head explain the sediment transport of coarse-grained sediment into Baffin Island fjords (Fig. 4; Syvitski and Normandeau, 2023). In Frobisher Bay, the Si–Sr–Zr–Fe–Ti sediment-rich seafloor is supplied by erosion of proglacial material (such as monzogranite-derived till) and remobilization of postglacial mud (Deering et al., 2018; Forbes et al., 2018). In addition, even though anthropogenic activities from Iqaluit have an impact on contaminant inputs in Frobisher Bay (Bartley et al., 2024; Corminboeuf et al., 2021), our results indicate no enrichment in V, Zn or Fe. The absence or the negative correlation between trace metals and D_{90}, Si and Zr (Fig. 7a)

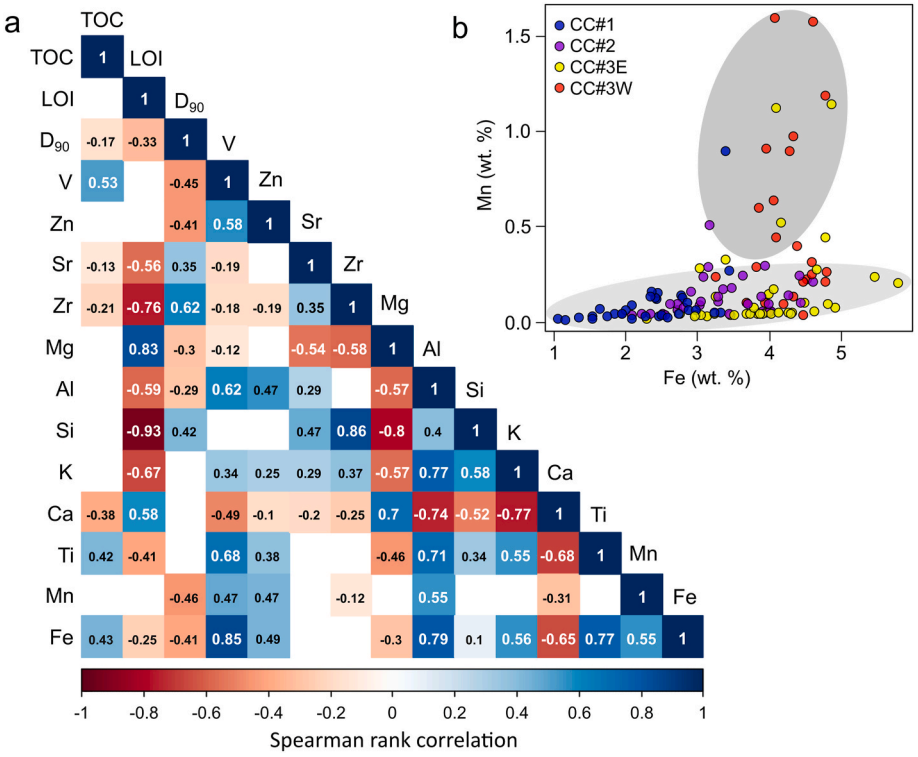

Fig. 7. a) Spearman rank correlation matrix of all variables measured in the study. The red squares represent significant negative correlations, the blue squares represent significant positive correlations, and the blank squares represent nonsignificant correlations. b) Correlation between Fe and Mn in the CA according to the provinces. Samples within the dark gray circle are mainly from the Amundsen Gulf and close to it, or from Baffin Bay. (For interpretation of the references to color in this figure legend, the reader is referred to the Web version of this article.)

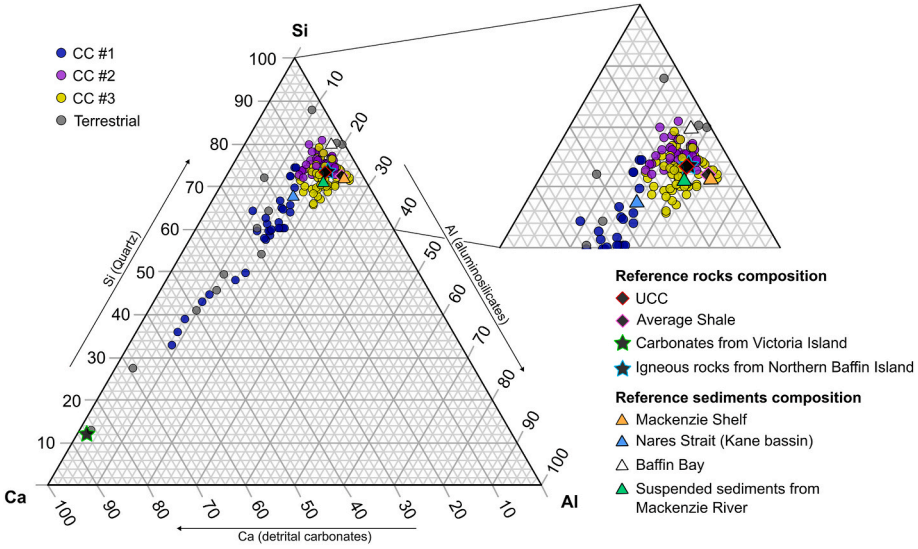

Fig. 8. Si–Ca–Al ternary plot of the marine and terrestrial samples. See Fig. 2 for comparative bedrock information and locations. The reference sediments are from Gamboa et al. (2017) for the Mackenzie Shelf, Caron et al. (2020) for Nares Strait, Loring (1984) for Baffin Bay and Dellinger et al. (2017) for suspended sediment samples from the Mackenzie River.

reveals that the relatively coarse sediments characterizing Frobisher Bay do not serve as effective carriers for trace metals and, therefore, do not favor their transport through the bay (Chen et al., 2016).

CC#3 is subdivided into two geographical zones: western and eastern CA. Even though substantially different sources and processes affect the zones, both are characterized by high TOC, trace metals and Fe contents and generally fine-grained sediments (Fig. 6). Most of the western CA subcluster is located within the Mackenzie River plume, and the latter represents the dominant source of sediment supply to the Canadian Beaufort Shelf (Fig. 8; Deschamps et al., 2018; Hill et al., 1991; Kutos et al., 2021; Gamboa et al., 2017). The sedimentary region is characterized by fine-grained sediments containing relatively high concentrations of Al–Fe–Mn–Ti and V–Zn–Cr, which can be related to clay minerals, such as kaolinite and illite (Deschamps et al., 2018; Myers and Darby, 2022), and Fe–Mn continental oxides derived from the Paleozoic to Mesozoic sedimentary rocks of the Mackenzie Valley

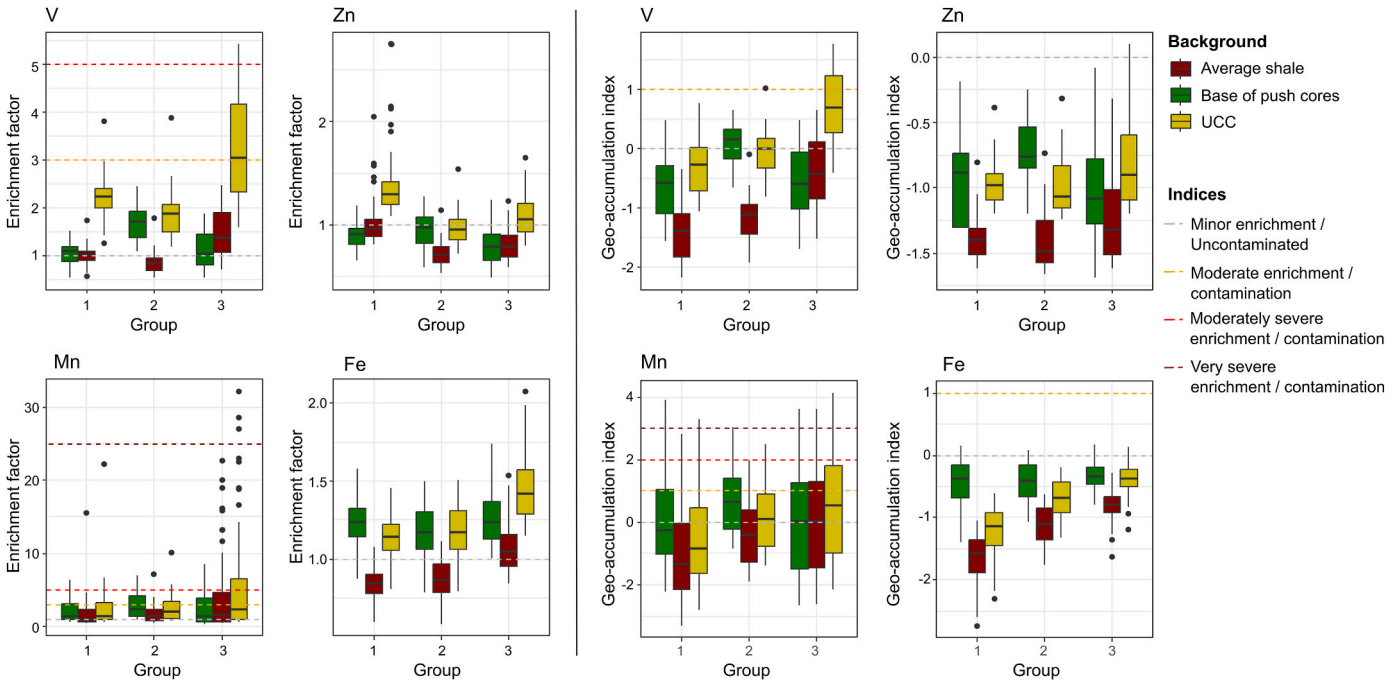

Fig. 9. Boxplots presenting the enrichment factor results and the geo-accumulation index of V, Zn, Mn and Fe. The boxplots are divided into three clusters and three boxes are shown per group, representing the three geochemical backgrounds used.

(Gamboa et al., 2017; Kutos et al., 2021; Harrison et al., 2011). These interpretations are consistent with the chemical end-member calculations derived from suspended sediment samples in the Mackenzie River Basin (Dellinger et al., 2017; Millot et al., 2003), suggesting that the primary source of the Mackenzie River sediments is the shales of the Interior Platform. Carbonates and calcareous shales (Fraser and Hutchison, 2017) and igneous rocks from the Bear Province (Fig. 2) also contribute significantly to the composition of the sediment. Likewise, significant abundances of magnetite (a Fe oxide mineral) are also found on the Mackenzie Shelf (Gamboa et al., 2017) and may result from the intrusive dikes on Banks Island (Myers and Darby, 2022). The high TOC content recorded in the sediments in western CA is mainly terrigenous, i.e., of petrogenic origin and from soils and wetlands, whereas the TOC from marine production accounts for a minor contribution (Drenzek et al., 2007). The organic material is mainly delivered by the Mackenzie River discharge (Goñi et al., 2013) which carry organic rich Devonian shale and coal material (Harrison et al., 2011; Yunker et al., 2011), and by coastal erosion of organic rich permafrost (Couture et al., 2018). A decreasing gradient in Al–Fe–Ti–V and TOC contents is observed in an overall W-E direction toward the Amundsen Gulf and toward Banks Island, confirming that the influence of the Mackenzie River plume is likely diluted eastward by other sedimentary processes, such as input from erosion of the coastal cliffs west of Banks Island (Gamboa et al., 2017). Mn concentrations are however showing an opposite trend, with the highest concentrations occurring in the Amundsen Gulf (Figs. 3 & 5b), indicating that other processes are influencing its distribution, such as different redox conditions near the sediment-water interface. Most Mn in the Arctic Ocean originates from rivers and coastal erosion, making the Mackenzie Shelf an area with very high inputs (MacDonald and Gobeil, 2012). However, high organic fluxes from the Mackenzie River maintain a shallow oxygen penetration depth (<2 cm; Magen, 2008), which leads to the reduction of Mn oxides close to the sediment-water interface and allows the dissolved Mn^{2+} to escape into the overlying waters (MacDonald and Gobeil, 2012). Particulate and dissolved Mn transported eastward by the Alaskan Coastal Current to the Amundsen Gulf and along the Banks Island coast are enriched in surface sediment because (1) the thicker oxygen penetration depth in the Amundsen Gulf (6 cm; Magen, 2008) allows the stability of the oxides at the surface and (2) below the oxic zone, reduced Mn diffuses upward and reprecipitates in the uppermost cm of sediment, causing surface enrichment. Surprisingly, there is stronger stratification and lower oxygenation of bottom waters in Amundsen Gulf and along Banks Island coast than the Beaufort Shelf (Magen, 2008; Reagan et al., 2024). The Mn enrichment observed in our dataset is thus attributed to the low oxygen consumption rates in the sediments resulting from low organic matter inputs (MacDonald and Gobeil, 2012; Magen, 2008; Magen et al., 2010).

The highest trace metal (V, Zn and Cr; Figs. 3 and 9) contents are found in the western CA subcluster, first because of important inputs from the Mackenzie River (Vonk et al., 2015) and second because of the presence of phase carriers (such clays, organic matter, Fe–Mn oxyhydroxides) that remove the dissolved trace metals from the water and scavenge them to the sediments. The Mackenzie River discharges high contents of fine-grained clay minerals, organic matter and Fe–Mn oxides. It is known that trace elements are preferentially retained in the fine fraction of sediment, as a relatively high specific surface area favors their sorption (Chen et al., 2016). However, the moderate negative correlation between D_{90}, and V and Zn highlights the association with clay minerals and reveals that other variables are influencing the distribution of metals, such as the sediment composition. Indeed, the adsorption of V and Zn onto Fe–Mn oxides, as well as their sorption/-complexation with organic matter, are important processes in the region (Jensen and Colombo, 2024). As shown by their positive correlation with Al (Fig. 7a), it is likely that these metals have a lithogenic provenance. However, because Mn is also strongly controlled by redox processes, its influence on trace metal distribution is limited. This observation aligns with findings from the Canadian Arctic waters, where particulate Fe and V, which correlate with particulate Al, are primarily controlled by lithogenic sources, whereas the distribution of particulate Mn is governed by oxidation conditions (Colombo et al., 2021; Jensen and Colombo, 2024).

High TOC concentrations primarily define the sediments from the eastern CA subcluster. This sedimentary region is distinct from the western CA region by a higher contribution of marine organic carbon

than terrestrial organic carbon (Goñi et al., 2013). The locations of the samples in northeast Baffin Bay correspond to the North Water Polynya and the Bylot Island–Lancaster Sound Polynyas (Stirling and Cleator, 1981; Hannah et al., 2009), a highly biologically productive region (Tremblay et al., 2012). The samples located close to Davis Strait exhibit lower but still higher-than-average TOC contents, indicating less biologically productive conditions. In addition to the relatively high concentrations of Si and Al, the sediments from this region are particularly characterized by high Fe and Ti content. Because Ti is not involved in any biological or redox processes, it principally indicates a terrigenous continental source, specifically when associated with Fe (Calvert and Pedersen, 2007). Several glaciers and icefields are present on Devon Island, Sirmilik National Park, SE Ellesmere Island (e.g., Manson and Prince of Wales Icefields) and west Greenland margin, and thus impact the sedimentation in these areas by generating sediment-laden meltwater plumes and iceberg rafting. These glaciers erode a mix of the Precambrian Canadian Shield composed of igneous rocks and gneiss, and the Arctic platform composed of sedimentary carbonate rocks, resulting in heterogeneous inputs composed of heavy minerals, quartz, K-feldspar, plagioclase and detrital carbonates (Marlowe, 1966).

Overall, low concentrations of Zn and V are observed in the eastern CA subcluster, despite high concentrations of Fe, Ti, and TOC (Figs. 3, 4 and 9). However, Jones Sound exhibits elevated V concentrations (150–228 μg/g), coinciding with the highest Fe and Mn content. The low V and Zn content measured in river and glacier samples from the north coast of Jones Sound (Fig. 3) suggest the absence of significant natural metal sources in the area. These concentrations are likely explained by increased scavenging enhanced by metal oxides.

Although Cr concentrations are mostly <DL, some samples display values between 100 and 135 μg/g in both the Canadian Beaufort Shelf and eastern CA regions (Fig. 3). These concentrations are twice as high as those reported in the Chukchi Sea region for the <160 μm sediment fraction (Cai et al., 2011) and higher than those reported in coastal and sound areas of northern Baffin Bay. However, these concentrations are comparable to those observed in deep-water mud from Baffin Bay (<50 μm; Campbell and Loring, 1980; Loring, 1984). In western CA, the highest concentrations are found close to the Mackenzie River mouth. Vonk et al. (2015) measured lower concentrations in channel and bank sediments of the Mackenzie Delta system (67–94 μg/g), but similar concentrations in shelf and lake sediments (96–141 μg/g) and suggest a depositional sorting pattern. This implies that there is an enrichment along the transect of fine particles (clay minerals, organic matter and metallic oxides) carrying metals such as Cr, leading to their deposition on the shelf and slope. In eastern CA, concentrations > DL are observed in central Nares Strait, outer Jones Sound, and northern Davis Strait. Terrestrial samples from the southern Ellesmere region consistently show low Cr concentrations. Thus, we infer that higher Cr scavenging by Fe–Mn oxides and organic matter drives its distribution in these areas.

5.2. Pollution indices

Pollution indices revealed no general enrichment or pollution of V or Zn in the CA sediments. However, EF and Igeo present divergent results depending on the geochemical background used. The difference is clearly visible for V enrichment (Fig. 9), for which the EF presents moderately severe enrichment in western CA, with UCC as background, while no enrichment is observed with local geochemical background. This highlights that the regional concentration in V is naturally high, most probably related to the discharge of the Mackenzie River, whose tributaries drain V-rich shales (Yukon Geological Survey, 2023; Yunker et al., 2011). Thus, the choice of background is an important variable that can significantly change the conclusions of a pollution study, and this is especially true in large spatial studies, such as those where bedrock geology varies greatly. The use of a local, onsite background is therefore more representative of the geological variability and natural concentration of the areas. The local background used in this study was associated with the chemical clusters identified with surface sediment data, and the difference between the background values of each cluster is significant. The V background concentration in CC#3 is indeed twice the values of the two other clusters. This highlights that the values from UCC or AS, which are usually suggested for normalization, are therefore far from the local background values in the CA.

Normalization is a method to consider the natural regional variability of trace metal content in sediment, like granulometric and mineralogical variations, to enable the identification and quantification of anthropogenic metal contributions (Loring, 1991). In the calculation of EFs, a normalizing element is used to compensate for these variations (Loring, 1991). Aluminum is commonly used for chemical normalization because it is a major element in marine sediments (generally composed of aluminosilicates). Additionally, it remains unaffected by biological, diagenetic, and anthropogenic processes (Boës et al., 2011). However, the use of a normalizing element has been criticized because its variability can be greater than that of the evaluated metal (Desaules, 2012; Poh and Tahir, 2017; Reimann and de Caritat, 2000, 2005). To evaluate this, EFs were also calculated with Ti as the normalizer, and the results were overall similar but noteworthy differences were identified for all the elements (Fig. S4b). Also, terrestrial sediment samples collected at southern Ellesmere Island have high EF values because of their low Al contents. The pollution classification of those sediments was very different from that of Igeo, which does not use a normalizing element (Fig. S4a). Thus, our results suggest that the use of EFs can lead to misinterpretation of contamination in the sediments if the reference metal/element ratio is not consistent with the natural background (e.g., Anderson and Kravitz, 2010; Poh and Tahir, 2017; Reimann and de Caritat, 2000, 2005; Van der Weijden, 2002).

Another factor to consider when the pollution indices values are interpreted, especially when deeper sediment values are used as a background, is the influence of early diagenesis and other geochemical processes (e.g., bottom scavenging within the nepheloid layer; Casse et al., 2019) within the sediment. Sediments at certain depths are naturally enriched or depleted in trace elements due to the dissolution and precipitation of redox host phases, such as Mn and Fe oxyhydroxides and sulfides (Kuzyk et al., 2017; Tribovillard et al., 2006). This phenomenon was observed in this study with respect to the Mn distribution, which presented severe enrichment in Amundsen Gulf sediments due to Mn remobilization and reprecipitation during early diagenesis. In this context, and to avoid misinterpretations stemming from early diagenesis, depth profiles of elemental concentrations in sediments and pore water should be used to provide essential information on the natural enrichment and depletion of trace elements required to assess anthropogenic influence (e.g., Trefry and Neff, 2019).

6. Conclusions

This study presents a vast geochemical survey of the Canadian Arctic, providing valuable new data on the chemical composition of surface sediment and new insights into the sedimentary dynamics of the region. The application of pollution indices in the assessment of sediment pollution was also studied to review the benefits and drawbacks of the method.

Geochemical data revealed a large regional variability in the seafloor composition of the CA, shaped by the regional bedrock geology. Three chemical clusters define the CA:

1) CC#1 (central CA) is dominated by high detrital carbonate content originating from the Arctic Platform though coastal erosion and sea ice transport.
2) CC#2 (southeastern CA: Queen Maud Gulf and the Baffin Island fjords and bays) is characterized by relatively coarse siliciclastic sediments influenced by small CA rivers and glaciers from Baffin Island eroding Canadian Shield rocks.

3) CC#3 (western and eastern CA) is characterized by sediments rich in TOC and Fe–Mn oxyhydroxides. The Western CA is highly influenced by the Mackenzie River discharge, containing high terrestrial organic carbon as well as lithogenic aluminosilicates and metallic oxides. The highest content of trace metals (V, Zn and Cr) are observed in this region and are associated with Fe–Mn oxides and clay minerals derived from the weathering of shales and siltstones that constitute the Mackenzie River Basin. In contrast, eastern CA is influenced by the high primary production of polynyas and glacial discharge from the surrounding glaciers of Devon and Ellesmere Islands.

Throughout the CA, the pollution indices suggest that trace metals originate from natural sources and pose a low ecological risk for benthic or other organisms living near the water-sediment interface. However, discrepancies were observed in the EF and Igeo results depending on the background used. Thus, those indices should be interpreted carefully. In addition, normalization of the metal data with a conservative element in the EF calculation also revealed several flaws. To avoid potential misinterpretations, it is recommended that EFs be validated with different conservative normalizing elements.

Finally, while pollution indices are useful for identifying elevated concentrations of trace elements, they should not be solely relied upon to assess metallic pollution or characterize human contributions in sediments. A regional geochemical survey, such as the one conducted in this study, combined with spatial variations in EFs and Igeo, provides a more comprehensive approach for understanding metal distribution, natural enrichment/depletion processes, and the impact of human activities on trace metal pollution.

CRediT authorship contribution statement

Camille Brice: Writing – original draft, Methodology, Investigation, Funding acquisition, Formal analysis, Data curation. **Jean-Carlos Montero-Serrano:** Writing – review & editing, Validation, Supervision, Resources, Investigation, Funding acquisition, Conceptualization. **Richard Saint-Louis:** Writing – review & editing, Supervision, Resources, Investigation, Conceptualization.

Declaration of competing interest

The authors declare that they have no known competing financial interests or personal relationships that could have appeared to influence the work reported in this paper.

Acknowledgments

We acknowledge the captains, officers, crews, and scientific participants of the 2016, 2017, 2018, 2019, and 2022 ArcticNet expeditions onboard CCGS Amundsen for the recovery of the sediment samples used in this study. We thank Claude Belzile (ISMER-UQAR), Dominique Lavallée (ISMER-UQAR), Agnieszka Adamowicz (UQAM-Geotop), and Jean-François Hélie (UQAM-Geotop) for providing technical support in the laboratory. This study was supported by ArcticNet (ArcticSeafloor project), Québec-Océan, Geotop, the Northern Scientific Training Program (NSTP), the Fonds de recherche du Québec - Nature et technologies (FRQNT) and the Natural Sciences and Engineering Research Council of Canada (NSERC) PhD scholarships provided to C. Brice, and NSERC Discovery Grants provided to J.-C. Montero-Serrano (RGPIN-2020-06600 and RGPNS-2020-06600). Finally, the authors thank one anonymous reviewer and John S. Armstrong-Altrin (National Autonomous University of Mexico) for their constructive reviews, which improved the quality of the manuscript, as well as Daniel S. Alessi and Zimeng Wang for their editorial work.

Appendix A. Supplementary data

Supplementary data to this article can be found online at https://doi.org/10.1016/j.apgeochem.2025.106432.

Data availability

All analytical data are archived in the PANGAEA database (https://doi.org/10.1594/PANGAEA.974731; https://doi.org/10.1594/PANGAEA.974727).

References

Aitchison, J., 1982. The statistical analysis of compositional data. J. Roy. Stat. Soc. B 44 (2), 139–160. https://rss.onlinelibrary.wiley.com/doi/abs/10.1111/j.2517-6161.1982.tb01195.x.

Alkire, M.B., Jacobson, A.D., Lehn, G.O., Macdonald, R.W., Rossi, M.W., 2017. On the geochemical heterogeneity of rivers draining into the straits and channels of the Canadian Arctic Archipelago. J. Geophys. Res.: Biogeosciences 122 (10), 2527–2547. https://agupubs.onlinelibrary.wiley.com/doi/abs/10.1002/2016JG003723.

AMAP, 1998. AMAP Assessment Report: Arctic Pollution Issues. Arctic Monitoring and Assessment Programme (AMAP), Oslo, Norway, p. xii+859.

AMAP, 2005. AMAP Assessment 2002: Heavy Metals in the Arctic. Arctic Monitoring and Assessment Programme (AMAP), Oslo, Norway, p. xvi+265.

AMAP, 2021a. AMAP Assessment 2020: POPs and Chemicals of Emerging Arctic Concern: Influence of Climate Change. Arctic Monitoring and Assessment Programme (AMAP), Tromsø, Norway viii+134 pp.

AMAP, 2021b. AMAP Assessment 2021: Mercury in the Arctic. Arctic Monitoring and Assessment Programme (AMAP), Tromsø, Norway, 324 pp.

Anderson, R.H., Kravitz, M.J., 2010. Evaluation of geochemical associations as a screening tool for identifying anthropogenic trace metal contamination. Environ. Monit. Assess. 167 (1), 631–641. https://doi.org/10.1007/s10661-009-1079-2.

Askari Dehno, M., Mousavi Harami, S.R., Noora, M.R., 2022. Environmental geochemistry of heavy metals in coral reefs and sediments of Chabahar Bay. Results Eng. 13, 100346. https://www.sciencedirect.com/science/article/pii/S2590123022000160.

Bartley, M.C., Tremblay, T., De Silva, A.O., Michelle Kamula, C., Ciastek, S., Kuzyk, Z.Z. A., 2024. Sedimentary records of contaminant inputs in Frobisher bay, Nunavut. Environ. Sci. Ecotechnol. 18, 100313. https://www.sciencedirect.com/science/article/pii/S2666498423000789.

Bédard, J., Hayes, B., Hryciuk, M., Beard, C., Williamson, N., Dell'Oro, T., et al., 2016. Geochemical database of Franklin sills, Natkusiak Basalts and shaler supergroup rocks, Victoria island, Northwest territories, and correlatives from Nunavut and the mainland. Geol. Surv. Can. Open File 8009 (1).

Belt, S.T., Vare, L.L., Massé, G., Manners, H.R., Price, J.C., MacLachlan, S.E., et al., 2010. Striking similarities in temporal changes to spring sea ice occurrence across the central Canadian Arctic Archipelago over the last 7000 years. Quat. Sci. Rev. 29 (25), 3489–3504. https://www.sciencedirect.com/science/article/pii/S0277379110002362.

Belzile, C., Montero-Serrano, J.-C., 2022. Quantifying simulated fine sand fraction in muddy sediment using laser diffraction. Can. J. Earth Sci. 59 (7), 455–461. https://cdnsciencepub.com/doi/abs/10.1139/cjes-2022-0011.

Birch, G.F., 2020. An assessment of aluminum and iron in normalisation and enrichment procedures for environmental assessment of marine sediment. Sci. Total Environ. 727, 138123. https://www.sciencedirect.com/science/article/pii/S0048969720316363.

Blott, S.J., Pye, K., 2001. GRADISTAT: a grain size distribution and statistics package for the analysis of unconsolidated sediments. Earth Surf. Process. Landf. 26 (11), 1237–1248.

Boës, X., Rydberg, J., Martinez-Cortizas, A., Bindler, R., Renberg, I., 2011. Evaluation of conservative lithogenic elements (Ti, Zr, Al, and Rb) to study anthropogenic element enrichments in lake sediments. J. Paleolimnol. 46 (1), 75–87. https://doi.org/10.1007/s10933-011-9515-z.

Borcard, D., Gillet, F., Legendre, P., 2011. Spatial analysis of ecological data. In: Numerical Ecology with R. Springer, pp. 227–292.

Brown, R.J.E., 1972. Permafrost in the Canadian Arctic Archipelago. Zeitschrift fur Geomorphologie 13, 102–130. https://cir.nii.ac.jp/crid/1570572699166533888.

Brown, K.A., Williams, W.J., Carmack, E.C., Fiske, G., François, R., McLennan, D., Peucker-Ehrenbrink, B., 2020. Geochemistry of small Canadian Arctic rivers with diverse geological and hydrological settings. J. Geophys. Res.: Biogeosciences 125 (1), e2019JG005414. https://agupubs.onlinelibrary.wiley.com/doi/abs/10.1029/2019JG005414.

Budko, D.F., Demina, L.L., Travkina, A.V., Starodymova, D.P., Alekseeva, T.N., 2022. The features of distribution of chemical elements, including heavy metals and Cs-137, in surface sediments of the Barents, Kara, Laptev and east Siberian seas. Minerals 12 (3), 328. https://www.mdpi.com/2075-163X/12/3/328.

Cai, M., Lin, J., Hong, Q., Wang, Y., Cai, M., 2011. Content and distribution of trace metals in surface sediments from the northern Bering Sea, Chukchi Sea and adjacent Arctic areas. Mar. Pollut. Bull. 63 (5–12), 523–527.

Calvert, S.E., Pedersen, T.F., 2007. Chapter fourteen elemental proxies for palaeoclimatic and palaeoceanographic variability in marine sediments: interpretation and

application. In: Hillaire–Marcel, C., De Vernal, A. (Eds.), Developments in Marine Geology, vol. 1. Elsevier, pp. 567–644.
Campbell, J.A., Loring, D.H., 1980. Baseline levels of heavy metals in the waters and sediments of Baffin Bay. Mar. Pollut. Bull. 11 (9), 257–261. https://www.sciencedirect.com/science/article/pii/0025326X80903148.
Canadian Ice Services, 2023. Annual Arctic Ice Atlas, Winter 2022-2023. Government of Canada, Ottawa.
Caron, M., Montero-Serrano, J.-C., St-Onge, G., Rochon, A., 2020. Quantifying provenance and transport pathways of holocene sediments from the Northwestern Greenland margin. Paleoceanogr. Paleoclimatol. 35 (5), e2019PA003809. https://agupubs.onlinelibrary.wiley.com/doi/abs/10.1029/2019PA003809.
Casse, M., Montero-Serrano, J.-C., St-Onge, G., Poirier, A., 2019. REE distribution and Nd isotope composition of estuarine waters and bulk sediment leachates tracing lithogenic inputs in eastern Canada. Mar. Chem. 211, 117–130. https://www.sciencedirect.com/science/article/pii/S0304420318302421.
Chen, Y.-M., Gao, J.-b., Yuan, Y.-Q., Ma, J., Yu, S., 2016. Relationship between heavy metal contents and clay mineral properties in surface sediments: implications for metal pollution assessment. Cont. Shelf Res. 124, 125–133. https://www.sciencedirect.com/science/article/pii/S0278434316303053.
Choudhary, S., Nayak, G.N., Khare, N., 2023. Sedimentary processes, metal enrichment and potential ecological risk of metals in lacustrine sediments of Svalbard, Arctic. Environ. Sci. Pollut. Control Ser. 30 (49), 106967–106981. https://doi.org/10.1007/s11356-022-23600-w.
Colombo, M., Brown, K.A., De Vera, J., Bergquist, B.A., Orians, K.J., 2019. Trace metal geochemistry of remote rivers in the Canadian Arctic Archipelago. Chem. Geol. 525, 479–491. https://www.sciencedirect.com/science/article/pii/S0009254119303742.
Colombo, M., Rogalla, B., Li, J., Allen, S.E., Orians, K.J., Maldonado, M.T., 2021. Canadian arctic Archipelago shelf-ocean interactions: a major iron source to Pacific derived waters transiting to the Atlantic. Glob. Biogeochem. Cycles 35 (10), e2021GB007058. https://agupubs.onlinelibrary.wiley.com/doi/abs/10.1029/2021GB007058.
Corminboeuf, A., Montero-Serrano, J.-C., St-Louis, R., 2021. Spatial and temporal distributions of polycyclic aromatic hydrocarbons in sediments from the Canadian Arctic Archipelago. Mar. Pollut. Bull. 171, 112729. https://www.sciencedirect.com/science/article/pii/S0025326X21007633.
Couture, N.J., Irrgang, A., Pollard, W., Lantuit, H., Fritz, M., 2018. Coastal erosion of permafrost soils along the Yukon coastal plain and fluxes of organic carbon to the Canadian Beaufort Sea. J. Geophys. Res.: Biogeosciences 123 (2), 406–422. https://agupubs.onlinelibrary.wiley.com/doi/abs/10.1002/2017JG004166.
Crecelius, E.A., Trefry, J.H., Steinhauer, M.S., Boehm, P.D., 1991. Trace metals in sediments from the inner continental shelf of the Western Beaufort Sea. Environ. Geol. Water Sci. 18 (1), 71–79. https://doi.org/10.1007/BF01704579.
Darby, D.A., Myers, W.B., Jakobsson, M., Rigor, I., 2011. Modern dirty sea ice characteristics and sources: the role of anchor ice. J. Geophys. Res.: Oceans 116 (C9). https://agupubs.onlinelibrary.wiley.com/doi/abs/10.1029/2010JC006675.
Deering, R., Misiuk, B., Bell, T., Forbes, D., Edinger, E., Tremblay, T., et al., 2018. Characterization of the seabed and postglacial sediments of inner Frobisher bay, Baffin island, Nunavut. Summary Activities 2018, Canada-Nunavut Geoscience Office 139–152.
Dellinger, M., Bouchez, J., Gaillardet, J., Faure, L., Moureau, J., 2017. Tracing weathering regimes using the lithium isotope composition of detrital sediments. Geology 45 (5), 411–414. https://doi.org/10.1130/G38671.1.
Déry, S.J., Stadnyk, T.A., MacDonald, M.K., Gauli-Sharma, B., 2016. Recent trends and variability in river discharge across northern Canada. Hydrol. Earth Syst. Sci. 20 (12), 4801–4818. https://hess.copernicus.org/articles/20/4801/2016/.
Desaules, A., 2012. Critical evaluation of soil contamination assessment methods for trace metals. Sci. Total Environ. 426, 120–131. https://www.sciencedirect.com/science/article/pii/S0048969712003968.
Deschamps, C.-E., Montero-Serrano, J.-C., St-Onge, G., 2018. Sediment provenance changes in the western Arctic Ocean in response to ice rafting, sea level, and oceanic circulation variations since the last deglaciation. G-cubed 19 (7), 2147–2165. https://agupubs.onlinelibrary.wiley.com/doi/abs/10.1029/2017GC007411.
Domingo, J.P.T., Ngwenya, B.T., Attal, M., David, C.P.C., Mudd, S.M., 2023. Geochemical fingerprinting to determine sediment source contribution and improve contamination assessment in mining-impacted floodplains in the Philippines. Appl. Geochem. 159, 105808. https://www.sciencedirect.com/science/article/pii/S0883292723002536.
Drenzek, N.J., Montluçon, D.B., Yunker, M.B., Macdonald, R.W., Eglinton, T.I., 2007. Constraints on the origin of sedimentary organic carbon in the Beaufort Sea from coupled molecular 13C and 14C measurements. Mar. Chem. 103 (1), 146–162. https://www.sciencedirect.com/science/article/pii/S0304420306001228.
Forbes, D.L., Bell, T., Manson, G.K., Couture, N.J., Cowan, B., Deering, R.L., et al., 2018. Chapter 8: coastal environments and drivers. From Science to Policy in the Eastern Canadian Arctic: an Integrated Regional Impact Study (IRIS) of Climate Change and Moderization, vol. 560. ArcticNet, Quebec City, p. 211.
Fraser, T., Hutchison, M.P., 2017. Lithogeochemical characterization of the middle–upper devonian road river group and canol and imperial formations on trail river, east richardson mountains, yukon: age constraints and a depositional model for fine-grained strata in the lower paleozoic richardson trough. Can. J. Earth Sci. 54 (7), 731–765. https://doi.org/10.1139/cjes-2016-0216.
Gamboa, A., Montero-Serrano, J.-C., St-Onge, G., Rochon, A., Desiage, P.-A., 2017. Mineralogical, geochemical, and magnetic signatures of surface sediments from the Canadian Beaufort shelf and Amundsen gulf (Canadian Arctic). G-cubed 18 (2), 488–512. https://agupubs.onlinelibrary.wiley.com/doi/abs/10.1002/2016GC006477.
Goñi, M.A., O'Connor, A.E., Kuzyk, Z.Z., Yunker, M.B., Gobeil, C., Macdonald, R.W., 2013. Distribution and sources of organic matter in surface marine sediments across the North American Arctic margin. Journal of Geophysical Research: Oceans 118 (9), 4017–4035. https://agupubs.onlinelibrary.wiley.com/doi/abs/10.1002/jgrc.20286.
Grenier, M., Brown, K.A., Colombo, M., Belhadj, M., Baconnais, I., Pham, V., et al., 2022. Controlling factors and impacts of river-borne neodymium isotope signatures and rare earth element concentrations supplied to the Canadian Arctic Archipelago. Earth Planet Sci. Lett. 578, 117341. https://www.sciencedirect.com/science/article/pii/S0012821X21005975.
Hakanson, L., 1980. An ecological risk index for aquatic pollution control.a sedimentological approach. Water Res. 14 (8), 975–1001. https://www.sciencedirect.com/science/article/pii/0043135480901438.
Hamel, D., Vernal, A.d., Gosselin, M., Hillaire-Marcel, C., 2002. Organic-walled microfossils and geochemical tracers: sedimentary indicators of productivity changes in the North Water and northern Baffin Bay during the last centuries. Deep Sea Res. Part II Top. Stud. Oceanogr. 49 (22), 5277–5295. https://www.sciencedirect.com/science/article/pii/S096706450200190X.
Hannah, C.G., Dupont, F., Dunphy, M., 2009. Polynyas and tidal currents in the Canadian arctic Archipelago. Arctic 62 (1), 83–95. http://www.jstor.org/stable/40513267.
Harrison, J.C., St-Onge, M.R., Petrov, O.V., Strelnikov, S.I., Lopatin, B.G., Wilson, F.H., Tella, S., Paul, D., Lynds, T.L., Shokalsky, S.P., Hults, C.K., Bergman, S., Jepsen, H.F., Solli, A., 2011. Geological map of the Arctic. Geological Survey of Canada, "A" Series Map, 2159A. Natural Resources Canada. https://doi.org/10.4095/287868.
Heginbottom, J.A.D., M, A., Harker, P.T., 1995. Canada, Permafrost (Cartographer).
Hélie, J.F., 2009. Elemental and stable isotopic approaches for studying the organic and inorganic carbon components in natural samples. IOP Conf. Ser. Earth Environ. Sci. 5 (1), 012005. https://doi.org/10.1088/1755-1307/5/1/012005.
Hill, P.R., Blasco, S.M., Harper, J.R., Fissel, D.B., 1991. Sedimentation on the Canadian Beaufort shelf. Cont. Shelf Res. 11 (8), 821–842. https://www.sciencedirect.com/science/article/pii/027843439190081G.
Hugelius, G., Strauss, J., Zubrzycki, S., Harden, J.W., Schuur, E.A.G., Ping, C.L., et al., 2014. Estimated stocks of circumpolar permafrost carbon with quantified uncertainty ranges and identified data gaps. Biogeosciences 11 (23), 6573–6593. https://bg.copernicus.org/articles/11/6573/2014/.
Jensen, L., Colombo, M., 2024. Shelf-basin connectivity drives dissolved Fe and Mn distributions in the western arctic ocean: a synoptic view into polar trace metal cycling. Oceanography (Wash. D. C.) 37 (2), 60–71. https://www.jstor.org/stable/27309822.
Kassambara, A., Mundt, F., 2020. Factoextra: extract and visualize the results of multivariate data analyses. R. Package Version 1.0.7. https://CRAN.R-project.org/package=factoextra.
Kondo, Y., Obata, H., Hioki, N., Ooki, A., Nishino, S., Kikuchi, T., Kuma, K., 2016. Transport of trace metals (Mn, Fe, Ni, Zn and Cd) in the western Arctic Ocean (Chukchi Sea and Canada basin) in late summer 2012. Deep Sea Res. Oceanogr. Res. Pap. 116, 236–252. https://www.sciencedirect.com/science/article/pii/S0967063716301765.
Kutos, O., Rochon, A., Montero-Serrano, J.-C., 2021. Evolution of palaeo-sea-surface conditions and sediment dynamics over the last 2700 years on the Mackenzie slope, Beaufort Sea (Canadian Arctic). Boreas 50 (3), 893–914. https://onlinelibrary.wiley.com/doi/abs/10.1111/bor.12513.
Kuzyk, Z.Z.A., Gobeil, C., Goñi, M.A., Macdonald, R.W., 2017. Early diagenesis and trace element accumulation in North American Arctic margin sediments. Geochem. Cosmochim. Acta 203, 175–200. https://www.sciencedirect.com/science/article/pii/S0016703716307128.
Lakeman, T.R., Pieńkowski, A.J., Nixon, F.C., Furze, M.F., Blasco, S., Andrews, J.T., King, E.L., 2018. Collapse of a marine-based ice stream during the early younger dryas chronozone, Western Canadian Arctic. Geology 46 (3), 211–214.
Lantuit, H., Overduin, P.P., Couture, N., Wetterich, S., Aré, F., Atkinson, D., et al., 2012. The Arctic coastal dynamics database: a new classification scheme and statistics on arctic permafrost coastlines. Estuaries Coasts 35 (2), 383–400. https://doi.org/10.1007/s12237-010-9362-6.
Lê, S., Josse, J., Husson, F., 2008. FactoMineR: an R package for multivariate analysis. J. Stat. Software 25 (1), 1–18. https://www.jstatsoft.org/index.php/jss/article/view/v025i01.
Lebeau, L.E., 2022. The Fury and Hecla geoscience project: whole rock and assay analysis from the Jungersen River area, northwestern Baffin island, Nunavut. Geoscience data series GDS2022-002. Canada-Nunavut Geosci. Office.
Letaïef, S., Montero-Serrano, J.C., St-Onge, G., 2021. Sedimentary processes within the Canadian Arctic Archipelago: relationships among sedimentological, geochemical, and magnetic sediment properties. G-cubed 22 (7), e2021GC009719.
Loring, D.H., 1984. Trace-metal geochemistry of sediments from Baffin bay. Can. J. Earth Sci. 21 (12), 1368–1378. https://cdnsciencepub.com/doi/abs/10.1139/e84-142.
Loring, D.H., 1991. Normalization of heavy-metal data from estuarine and coastal sediments. ICES (Int. Counc. Explor. Sea) J. Mar. Sci. 48 (1), 101–115. https://doi.org/10.1093/icesjms/48.1.101.
Macdonald, R.W., Bewers, J.M., 1996. Contaminants in the arctic marine environment: priorities for protection. ICES (Int. Counc. Explor. Sea) J. Mar. Sci. 53 (3), 537–563. https://doi.org/10.1006/jmsc.1996.0077.
Macdonald, R.W., Gobeil, C., 2012. Manganese sources and sinks in the Arctic Ocean with reference to periodic enrichments in basin sediments. Aquat. Geochem. 18 (6), 565–591. https://doi.org/10.1007/s10498-011-9149-9.
Magen, C., 2008. *Origin, Sedimentation and Diagenesis of Organic Matter in Coastal Sediments of the Southern Beaufort Sea region, Canadian Arctic.* (PhD). McGill University, Montreal.
Magen, C., Chaillou, G., Crowe, S.A., Mucci, A., Sundby, B., Gao, A., et al., 2010. Origin and fate of particulate organic matter in the Southern Beaufort Sea – Amundsen Gulf

region, Canadian Arctic. Estuar. Coast Shelf Sci. 86 (1), 31–41. https://www.sciencedirect.com/science/article/pii/S0272771409004351.
Marlowe, J.I., 1966. Mineralogy as an indicator of long-term current fluctuations in Baffin Bay. Can. J. Earth Sci. 3 (2), 191–201. https://cdnsciencepub.com/doi/abs/10.1139/e66-015.
McLaughlin, F., Shimada, K., Carmack, E., Itoh, M., Nishino, S., 2005. The hydrography of the southern Canada Basin, 2002. Polar Biol. 28 (3), 182–189. https://doi.org/10.1007/s00300-004-0701-6.
McMartin, I., Berman, R., Normandeau, P., Percival, J., 2013. Till composition of a transect across the Thelon tectonic zone, queen Maud block, and adjacent Rae craton: results from the geo-mapping frontiers' chantrey project. Geol. Surv. Can. Open File 7418, 22.
Millot, R., Gaillardet, J.é., Dupré, B., Allègre, C.J., 2003. Northern latitude chemical weathering rates: clues from the Mackenzie River Basin, Canada. Geochem. Cosmochim. Acta 67 (7), 1305–1329. https://www.sciencedirect.com/science/article/pii/S0016703702012073.
Müller, G., 1969. Index of geoaccumulation in sediments of the rhine river. Geojournal 2, 108–118.
Myers, W.B., Darby, D.A., 2022. A compilation of the silt and clay mineralogy from coastal and shelf regions of the Arctic Ocean. Mar. Geol. 454, 106948. https://www.sciencedirect.com/science/article/pii/S0025322722002195.
Naidu, A.S., Blanchard, A.L., Misra, D., Trefry, J.H., Dasher, D.H., Kelley, J.J., Venkatesan, M.I., 2012. Historical changes in trace metals and hydrocarbons in nearshore sediments, Alaskan Beaufort Sea, prior and subsequent to petroleum-related industrial development: Part I. Trace metals. Mar. Pollut. Bull. 64 (10), 2177–2189. https://www.sciencedirect.com/science/article/pii/S0025326X1200358X.
Normandeau, A., Dietrich, P., Hughes Clarke, J., Van Wychen, W., Lajeunesse, P., Burgess, D., Ghienne, J.-F., 2019. Retreat pattern of glaciers controls the occurrence of turbidity currents on high-latitude fjord deltas (eastern Baffin island). J. Geophys. Res.: Earth Surf. 124 (6), 1559–1571. https://agupubs.onlinelibrary.wiley.com/doi/abs/10.1029/2018JF004970.
O'Brien, M.C., Macdonald, R.W., Melling, H., Iseki, K., 2006. Particle fluxes and geochemistry on the Canadian Beaufort Shelf: implications for sediment transport and deposition. Cont. Shelf Res. 26 (1), 41–81. https://www.sciencedirect.com/science/article/pii/S0278434305002001.
O'Donnell, J.A., Carey, M.P., Koch, J.C., Baughman, C., Hill, K., Zimmerman, C.E., et al., 2024. Metal mobilization from thawing permafrost to aquatic ecosystems is driving rusting of Arctic streams. Commun. Earth Environ. 5 (1), 268. https://doi.org/10.1038/s43247-024-01446-z.
Palarea-Albaladejo, J., Martín-Fernández, J.A., 2013. Values below detection limit in compositional chemical data. Anal. Chim. Acta 764, 32–43. https://www.sciencedirect.com/science/article/pii/S0003267012018363.
Palarea-Albaladejo, J., Martín-Fernández, J.A., 2015. zCompositions — R package for multivariate imputation of left-censored data under a compositional approach. Chemometr. Intell. Lab. Syst. 143, 85–96. https://www.sciencedirect.com/science/article/pii/S0169743915000490.
Poh, S.-C., Tahir, N.M., 2017. The common pitfall of using enrichment factor in assessing soil heavy metal pollution. Malays. J. Anal. Sci. 21, 52–59.
R Core Team, 2024. R: A language and environment for statistical computing. R Foundation for Statistical Computing, Vienna, Austria.
Reagan, J.R.B., Tim, P., García, Hernán E., Locarnini, Ricardo A., Baranova, Olga K., Bouchard, Courtney, Cross, Scott L., Mishonov, Alexey V., Paver, Christopher R., Seidov, Dan, Wang, Zhankun, Dukhovskoy, Dmitry, 2024. World Ocean Atlas 2023. NOAA National Centers for Environmental Information. Dataset. NCEI Accession 0270533.
Reimann, C., de Caritat, P., 2000. Intrinsic flaws of element enrichment factors (EFs) in environmental geochemistry. Environ. Sci. Technol. 34 (24), 5084–5091. https://doi.org/10.1021/es001339o.
Reimann, C., de Caritat, P., 2005. Distinguishing between natural and anthropogenic sources for elements in the environment: regional geochemical surveys versus enrichment factors. Sci. Total Environ. 337 (1), 91–107. https://www.sciencedirect.com/science/article/pii/S0048969704004760.
Reimnitz, E., Clayton, J.R., Kempema, E.W., Payne, J.R., Weber, W.S., 1993. Interaction of rising frazil with suspended particles: tank experiments with applications to nature. Cold Reg. Sci. Technol. 21 (2), 117–135. https://www.sciencedirect.com/science/article/pii/0165232X9390002P.
Ribeiro, S., Limoges, A., Massé, G., Johansen, K.L., Colgan, W., Weckström, K., et al., 2021. Vulnerability of the North Water ecosystem to climate change. Nat. Commun. 12 (1), 4475. https://doi.org/10.1038/s41467-021-24742-0.
Rothwell, R., Croudace, I., 2015. Twenty years of XRF core scanning marine sediments: what do geochemical proxies tell us? In: Croudace, I., Rothwell, R. (Eds.), Micro-XRF Studies of Sediment Cores: Applications of a Non-destructive Tool for the Environmental Sciences. Springer, Dordrecht, pp. 25–102. Netherlands.
St-Hilaire-Gravel, D., Forbes, D.L., Bell, T., 2012. Multitemporal analysis of a gravel-dominated coastline in the central Canadian arctic Archipelago. J. Coast Res. 28 (2), 421–441. https://doi.org/10.2112/JCOASTRES-D-11-00020.1.
Steele, M., Morison, J., Ermold, W., Rigor, I., Ortmeyer, M., Shimada, K., 2004. Circulation of summer Pacific halocline water in the Arctic Ocean. J. Geophys. Res.: Oceans 109 (C2). https://agupubs.onlinelibrary.wiley.com/doi/abs/10.1029/2003JC002009.
Stein, R., Macdonald, R.W., 2004. The Organic Carbon Cycle in the Arctic Ocean.
Stirling, I., Cleator, H., 1981. Polynyas in the Canadian Arctic. Canadian Wildlife Service, Ottawa (Occasional Paper Number 45).
Syvitski, J., Normandeau, A., 2023. Sediment redistribution processes in Baffin Island fjords. Mar. Geol. 458, 107024. https://www.sciencedirect.com/science/article/pii/S0025322723000361.
Taylor, S.R., McLennan, S.M., 1985. The Continental Crust: its Composition and Evolution. Blackwell Scientific Pub., United States. Palo Alto, CA.
Thompson, M., Ellison, S.L.R., Wood, R., 2002. Harmonized guidelines for single-laboratory validation of methods of analysis (IUPAC Technical Report). Pure Appl. Chem. 74 (5), 835–855. https://doi.org/10.1351/pac200274050835.
Trefry, J.H., Neff, J.M., 2019. Effects of offshore oil exploration and development in the Alaskan Beaufort Sea: a three-decade record for sediment metals. Integrated Environ. Assess. Manag. 15 (2), 209–223. https://setac.onlinelibrary.wiley.com/doi/abs/10.1002/ieam.4069.
Tremblay, J.-É., Robert, D., Varela, D.E., Lovejoy, C., Darnis, G., Nelson, R.J., Sastri, A.R., 2012. Current state and trends in Canadian Arctic marine ecosystems: I. Primary production. Clim. Change 115 (1), 161–178. https://doi.org/10.1007/s10584-012-0496-3.
Trettin, H., Bally, A., Palmer, A., 1989. The Arctic Islands. Geological Society of America.
Tribovillard, N., Algeo, T.J., Lyons, T., Riboulleau, A., 2006. Trace metals as paleoredox and paleoproductivity proxies: an update. Chem. Geol. 232 (1), 12–32. https://www.sciencedirect.com/science/article/pii/S000925410600132X.
Turekian, K.K., Wedepohl, K.H., 1961. Distribution of the elements in some major units of the earth's crust. GSA Bulletin 72 (2), 175–192. https://doi.org/10.1130/0016-7606(1961)72[175:DOTEIS]2.0.CO;2.
van den Boogaart, K.G., Tolosana-Delgado, R., 2008. "compositions": A unified R package to analyze compositional data. Comput. Geosci. 34 (4), 320–338. https://www.sciencedirect.com/science/article/pii/S009830040700101X.
Van der Weijden, C.H., 2002. Pitfalls of normalization of marine geochemical data using a common divisor. Mar. Geol. 184 (3), 167–187. https://www.sciencedirect.com/science/article/pii/S0025322701002973.
Vincent, R.F., 2023. An assessment of the lancaster sound polynya using satellite data 1979 to 2022. Remote Sens. 15 (4), 954. https://www.mdpi.com/2072-4292/15/4/954.
Viscosi-Shirley, C., Mammone, K., Pisias, N., Dymond, J., 2003. Clay mineralogy and multi-element chemistry of surface sediments on the Siberian-Arctic shelf: implications for sediment provenance and grain size sorting. Cont. Shelf Res. 23 (11), 1175–1200. https://www.sciencedirect.com/science/article/pii/S0278434303000918.
Vonk, J.E., Giosan, L., Blusztajn, J., Montlucon, D., Graf Pannatier, E., McIntyre, C., et al., 2015. Spatial variations in geochemical characteristics of the modern Mackenzie Delta sedimentary system. Geochem. Cosmochim. Acta 171, 100–120. https://www.sciencedirect.com/science/article/pii/S0016703715004998.
Wei, T., Simko, V., Levy, M., Xie, Y., Jin, Y., Zemla, J., 2017. Package 'corrplot'. Statistician 56 (316), e24.
Yukon Geological Survey, 2023. Yukon Lithogeochemistry data set. From Yukon Geological Survey. https://data.geology.gov.yk.ca/Compilation/35.
Yunker, M.B., Macdonald, R.W., Snowdon, L.R., Fowler, B.R., 2011. Alkane and PAH biomarkers as tracers of terrigenous organic carbon in Arctic Ocean sediments. Org. Geochem. 42 (9), 1109–1146. https://www.sciencedirect.com/science/article/pii/S0146638011001641.
Zhang, T., Wang, R., Xiao, W., Polyak, L., Astakhov, A., Dong, L., et al., 2021. Characteristics of terrigenous components of Amerasian Arctic Ocean surface sediments: implications for reconstructing provenance and transport modes. Mar. Geol. 437, 106497. https://www.sciencedirect.com/science/article/pii/S0025322721000797.